Manipulating Mitochondrial Integrity in a Parkinson's Disease Model

Jingwei Chen

Thesis submitted to the University of Ottawa in partial fulfillment of the requirements for the M.Sc. program in Cellular and Molecular Medicine

Department of Cellular and Molecular Medicine
Faculty of Medicine
University of Ottawa

ABSTRACT

Mitochondrial dysfunction has been identified as a key factor in the progression of Parkinson's disease. Mitochondrial dysfunction has been shown to induce stress pathways, leading to neuronal dysfunction and cell death. Our lab has previously identified that, in neurons, reconfiguring the mitochondria using supercomplex assembly factors is protective against excitotoxic stress. For this thesis, we sought to characterize the stress pathways and synaptic impairment in an *in vitro* mitochondrial dysfunction model. Then, to determine if we can rescue the deficits shown, we manipulated mitochondrial integrity using the inner mitochondrial membrane targeted isoform of MCL1, which has previously been shown to regulate cristae structure and mitochondrial supercomplex assembly. We demonstrate that the integrated stress response is activated upon mitochondrial dysfunction. Next, we show mitochondrial dysfunction leads to a downregulation of synaptic genes involved in neurotransmission. Finally, our results show that both the anti-apoptotic outer mitochondrial membrane-targeted isoform, and MCL1-Matrix are able to prevent cell death in response to mitochondrial dysfunction; however, MCL1-Matrix confers greater reduction in ISR activation and reactive oxygen species production. These data suggest that manipulating mitochondrial integrity, using MCL1-Matrix, confers a broad protective effect against neuronal stressors and may be used as a novel approach to preventing Parkinson's disease.

LIST OF FIGURES

LIST OF TABLES

LIST OF ABBREVIATIONS

6-OHDA	6-Hydroxydopamine
AAC1	ATP/ADP Carrier 1
AD	Alzheimer's Disease
AIF	Apoptosis Inducing Factor
ANOVA	Analysis of Variance
ANT1	Adenine Nucleotide Transporter 1
Apaf1	Apoptotic Peptidase Activating Factor 1
αSyn	α-Synuclein
ATF4	Activating Transcription Factor 4
ATP	Adenosine Triphosphate
BCL2	B-Cell Lymphoma 2
bGH	Bovine Growth Hormone
Ca^{2+}	Calcium Ion
CAD	Caspase-Activated DNAse
Chac1	ChaC Glutathione Specific Gamma-Glutamylcyclotransferase 1
CHOP	C/EBP homologous protein
CO_2	Carbon Dioxide
CoQ	Coenzyme Q
COX7RP	Cytochrome c Oxidase Subunit 7A-Related Protein
DA	Dopaminergic
DJ-1	Protein Deglycase
DMEM	Dulbecco's Modified Eagle's Medium
DMSO	Dimethyl Sulfoxide
DNA	Deoxyribonucleic Acid
DRP1	Dynamin-related Protein 1
EDTA	Ethylenediaminetetraacetic Acid
eIF2α	Eukaryotic Translation Initiation Factor 2α
ER	Endoplasmic Reticulum
ETC	Electron Transport Chain
$FADH_2$	Reduced Flavin Adenine Dinucleotide
FBS	Fetal Bovine Serum
GADD34	Growth Arrest and DNA Damage-Inducible Protein
GC	Genomic Content
GFP	Green Fluorescent Protein
HEK293T	Human Embryonic Kidney 293T
HIG2A	HIG1 Hypoxia Inducible Domain Family Member 2A
IAP	Inhibitor of Apoptosis Proteins
IMM	Inner Mitochondrial Membrane
ISR	Integrated Stress Response
L-DOPA	Levodopa
MCL1	Myeloid Cell Leukemia-1
MFN1	Mitofusin 1
MFN2	Mitofusin 2
mL	Millilitre
mM	Millimolar

MOI	Multiplicity of Infection
MPTP	1-Methyl-4-phenyl-1,2,3,6-tetrahydrophyridine
MPP^+	Methyl-4-phenylpyridinium
mtDNA	Mitochondrial DNA
NADH	Reduced Nicotinamide Adenine Dinucleotide
ng	Nanograms
NSF	*N*-ethylmaleimide-sensitive Factor
OM	Outer Membrane
OMM	Outer Mitochondrial Membrane
OPA1	Optic Atrophy 1
OXPHOS	Oxidative Phosphorylation
PBS	Phosphate-Buffered Saline
PCR	Polymerase Chain Reaction
PD	Parkinson's Disease
PEI	Polyethyleneimine
PES	Polyethersulfone
PINK1	PTNE-Induced Kinase 1
PolG	Polymerase γ
PTEN	Protein Phosphatase and Tensin Homolog
PTP	Permeability Transition Pore
PUMA	p53 Upregulated Mediator of Apoptosis
PVDF	Polyvinylidene Fluoride
rAAV	Recombinant Adeno-Associated Virus
RIPA	Radioimmunoprecipitation Assay Buffer
RNA	Ribonucleic Acid
ROS	Reactive Oxygen Species
RT-qPCR	Real Time Quantitative PCR
shCtrl	Scramble Control Virus
shOPA1	OPA1 Knockdown Virus
Slc7a11	Solute Carrier Family 7 Member 11
SN	Substantia Nigra
SNAP	Synaptosomal-Associated Protein
SNARE	Soluble NSF Attachment Protein Receptor
SYT	Synaptotagamin
TBS	Tris-Buffered Saline
TBST	Tris-Buffered Saline with 0.1% Tween 20
Trib3	Tribbles Homologue 3
TU	Transduction Units
µg	Microgram
µL	Microlitre
µm	Micrometre
µM	Micromolar

ACKNOWLEDGEMENTS

First and foremost, I would like to thank my supervisor, Dr. Ruth Slack, whose patience, knowledge, and overflowing positivity supported me through my MSc thesis project. Without her excellent guidance and feedback, I would not be half the scientist I am today.

I would also like to extend my deepest appreciation to all the past and present members of the Slack lab: Smitha Paul, Dr. Imane Chakroum, Dr. Yubing Liu, Dr. Bensun Fong, Mohammed Ariff Iqbal, Maria Bilen, Vanessa Jabr, Monica Nguyen, Amaal Abdullahi Abdi, Daniel O'Neil, Marie-Michelle McNicoll, and Eric Zorbas. I hope that I was able to give back to the lab even a fraction of what I gained. I sincerely thank our lab manager, Smitha Paul, for her dedication and assistance. I wish to sincerely thank Mohamed Ariff Iqbal for all his help training, problem solving, and working alongside me. I wish to thank Dr. Bensun Fong, for all the scintillating conversations that we had, along with the bioinformatics data used in this thesis. I would like to thank Dr. Yubing Liu, for all the conversations, technical knowledge, and food that she imparted me. I would like to thank Maria Bilen for the interesting conversations we had and for the bioinformatics and qPCR data used in this thesis.

I would like to sincerely thank my thesis advisory committee members Dr. Maxime Rousseaux and Dr. Stephen Ferguson for their insight. I am grateful for their guidance and time throughout this project.

I am very grateful for the support of many individuals at Roger Guidon Hall. I would like to thank Steve Callaghan and Terry Suk from the Rousseaux lab and Dr. James Taylor from the GEM core for their assistance with AAV cloning and Dr. Jungwoo Yang from the Chen lab for his guidance with AAV production. I would also like to thank Dr. Dianbo Qu from the Jahani lab for

his guidance with the MitoSOX experiments. I would also like to thank Dr. Chloë van Oostende-Triplet and Dr. Ian Blum from the Cell Biology and Image Acquisition Core for all their assistance. Finally, I would like to thank the best lab neighbours, Harper lab, in particular Dr. Chantal Pileggi, Gaganvir Parmar, Claire Fong-McMaster, Nina Hadzimustafic, and Briana Hooks, for feeding and tolerating me. It was fun.

I would also like to acknowledge the financial support from the Krembil Foundation at Brain Canada and Canadian Institutes of Health Research (CIHR).

Finally, I would like to thank my family for their unwavering support. I would most likely not be alive without them.

INTRODUCTION

1.1 Overview of Parkinson's Disease

1.1.1 Pathology and Clinical Aspects of Parkinson's Disease

Parkinson's disease (PD) is a progressive neurodegenerative condition characterized by a loss of dopaminergic (DA) neurons in the Substantia Nigra (SN) within the basal ganglia. The most common characteristic is the formation of Lewy bodies made of α-synuclein (αSyn) protein aggregates (Armstrong and Okun, 2020). Due to the dopamine depletion, patients show motor symptoms such as resting tremor, bradykinesia, and a mask-like face, and non-motor symptoms, such as sleep disturbances and, gastric and urinary disorders (Okun, 2012; Rodriguez-Sanchez *et al*., 2021). As the disease progresses, the motor symptoms become more pronounced and patients may begin to show cognitive and psychological decline, such as dementia, depression, and anxiety (Bereckzi *et al.*, 2018). Most incidences of PD are sporadic and are thought to be due to interactions between genetic susceptibility and environmental causes, with certain genes known to be inheritable risk factors (Subramaniam and Chesselet, 2013). While the causes may be complex, PD cases and models do appear to share certain similarities, such as mitochondrial dysfunction, increase in oxidative stress, or impairments in cellular respiration. There is currently no cure for PD; the current therapies available, such as dopamine replacement therapies and deep brain stimulation, only alleviate motor symptoms (Armstrong and Okun, 2020; Servello *et al*., 2016). Furthermore, neither therapy prevents or slows the progression of PD, thus, a therapy that can prevent or delay PD progression is necessary.

1.1.2 Structural deficits in PD

The basal ganglia are a group of nuclei which lie below the cerebral cortex and is comprised of the striatum, globus pallidus, and the SN (Obeso *et al*., 2008). The basal ganglia have typically been associated with smoothing movements by regulating thalamic and cortical activity; thus, any issues in the basal ganglia are typically associated with motor disorders such as PD and Huntington's disease. Furthermore, the basal ganglia projects to other areas of the brain, such as the limbic system and non-motor areas of the cortex, which may explain the non-motor, cognitive, and psychological disturbances in PD patients (Lanciego *et al*., 2012). Multiple circuits are used to refine movement with inputs arriving from the cortex and the SN (Gerfen and Surmeier, 2011). The information is passed from the striatum to the globus pallidus, then to the thalamus, before arriving again at the cortex, and involves the coordination of excitatory and inhibitory neurotransmitter systems. The SN neurons typically modulate this pathway with dopamine, which may be excitatory or inhibitory, depending on the circuit. Upon PD diagnosis and appearance of motor symptoms, it is estimated that 50-70% of DA neurons from the SN are already lost, leading to dysregulation of these circuits (Cheung *et al*., 2010). This dysregulation could be modulated through the administration of levodopa in a monkey model (Papa *et al*., 1999). Furthermore, PD-associated neuronal loss has been observed in in other regions, such as the locus coeruleus in the brain stem, ventral tegmental area of the midbrain, and thalamus (Bertrand *et al*., 1997; McRitchie *et al*., 1997; Henderson *et al*., 2000). Many studies have sought to examine why DA neurons of the SN are particularly vulnerable to environmental stressors. Recently, it has been reported that these neurons have high basal energy requirements leading to elevated levels of basal oxidative stress and a reduced ability to cope (Pacelli *et al*., 2015).

1.1.3 Mitochondrial Dysfunction in Aging and Genetic Risk Factors in PD

While the underlying cause of PD progression is yet to be elucidated, many studies have identified mitochondrial dysfunction as a key contributor of PD development. (**Fig 1**). Parkin and protein phosphatase and tensin homolog (PTEN)-induced kinase 1 (PINK1) are proteins that regulate mitophagy and have been found to be mutated in familial PD (Matsuda *et al*., 2010; Hattori *et al*., 1998; Valente *et al*., 2002). Mitophagy is a process where damaged mitochondria are identified and are marked for removal by autophagy (Matsuda *et al*., 2010). PINK1, which is normally degraded in cells with healthy mitochondria, is stabilized by damaged ones and accumulates on the outer mitochondrial membrane (OMM) (Narendra *et al*., 2010; Matsuda *et al*., 2010). Parkin, an E3 ubiquitin ligase, is recruited by PINK1 accumulation, and tags the mitochondria for autophagy (Matsuda *et al*., 2013). Mutations in PINK1 and Parkin and the subsequent disruption of mitophagy leads to the accumulation of dysfunctional mitochondria, underscoring the importance of mitochondria in PD progression. During aging, one of the most important risk factors for sporadic PD, there is a natural age-dependent formation of Lewy bodies and loss of neurons in SNc (Buchman *et al*., 2012). Furthermore, there is a decline in mitochondrial function leading to increased reactive oxygen species (ROS) production, accumulation of mitochondrial DNA (mtDNA) mutations, and impaired oxidative phosphorylation (OXPHOS) (Grünewald *et al*., 2019; Khacho et al., 2019). In post-mortem samples of patients with PD, there were high levels of mtDNA deletions, many of which coded for proteins associated with mitochondrial respiration (Bender *et al*., 2006). Proofreading mutations in the mitochondrial DNA polymerase γ (PolG), crossed with a Parkin knockout, have been used to simulate an accelerated aging model, which lead to deficits in OXPHOS complexes and DA neuron dysfunction (Dai *et al*., 2013; Pickrell *et al*., 2015). Furthermore, a post-mortem analysis of humans with PolG mutations showed a decrease in complex I and IV expression, increased presence of α-Synuclein,

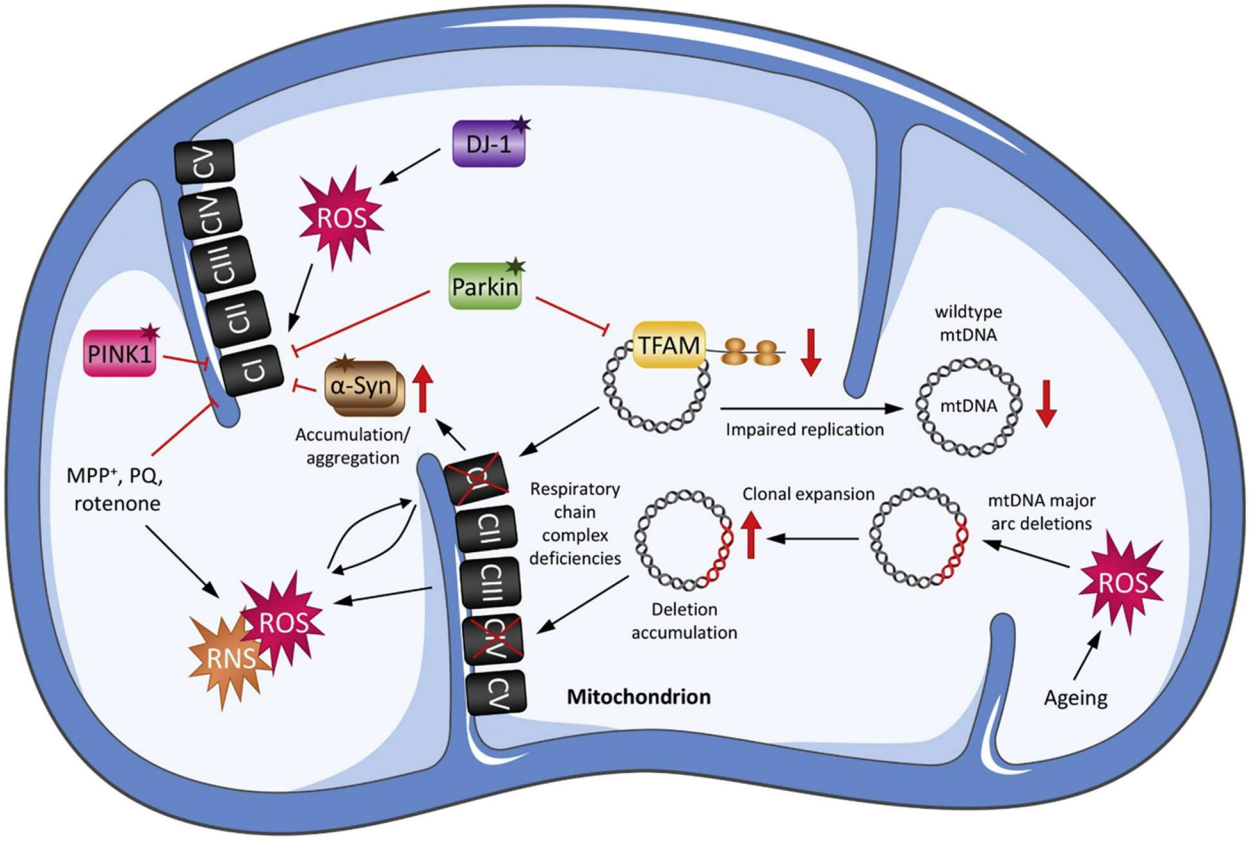

Fig 1. Mitochondrial dysfunction is associated with PD progression. Multiple genetic causes and neurotoxins have been used to induce mitochondrial dysfunction and model PD. Aging is associated with mtDNA damage, leading to mutations in important proteins in the ETC. Mitophagy has also been shown to be impaired with Parkin/PINK1 mutations, leading to the accumulation of dysfunctional mitochondria. Neurotoxins, which produce parkinsonism, impair complex I leading to oxidative stress and cell death. Adapted from Grünewald *et al*. (2019).

and more severe DA neuron loss in the SN (Reeve *et al*., 2013). Loss of protein deglycase (DJ-1), which has been shown to regulate the antioxidant response, has been associated with recessive familial parkinsonism (Aleyasin *et al*., 2010; Bonifati *et al*., 2003). DA neurons lacking DJ-1 were found to have elevated mitochondrial oxidative stress and increased αSyn accumulation, which were rescued with mitochondrial-targeted antioxidants (Burbella *et al*., 2017). Parkinsonism due to mutations in mitochondrial dynamics-regulating proteins have also been observed and will be explored later in this dissertation.

1.1.4 Mitochondrial Dysfunction is Induced by Neurotoxic Models of PD

Another common method to investigate the cellular mechanisms involved in DA neuron death is the use of neurotoxins, which induce mitochondrial dysfunction and Parkinson-like symptoms (Chia *et al*., 2020). 6-Hydroxydopamine (6-OHDA) has been used in both *in vitro* and *in vivo* PD models (Demmings *et al*., 2020; Perese *et al*., 1989). When injected into the SN, it oxidizes and produces ROS, leading to death of DA neurons (Perese *et al*., 1989). 6-OHDA, however, does not show Lewy Body formation. Rotenone and 1-methyl-4-phenyl-1,2,3,6-tetrahydropyridine (MPTP) both cause mitochondrial dysfunction through the inhibition of complex I in mitochondrial respiration (Li *et al*., 2003; Shishido *et al*., 2019). Rotenone treatment has been shown to increase ROS, and when intraperitonially, lead to a decrease in DA neurons and cause Lewy body formation (Li *et al*., 2003; Inden *et al*., 2011; Zhang *et al*., 2022). MPTP is selectively taken up by DA neurons through the dopamine transporter and oxidized into methyl-4-phenylpyridinium (MPP^+) (Javitch *et al*., 1985; Martí *et al*., 2017). MPP^+ then acts in a similar fashion to rotenone, leading to increased ROS and loss of DA neurons but does not show formation of Lewy bodies (Inden *et al*, 2011; Zhang *et al*., 2022). Paraquat is another neurotoxin that has

been used as a PD model. Paraquat alters glutathione levels, leading to the formation of ROS and subsequent cell death (Kang *et al*., 2009; Niso-Santano *et al*., 2010).

1.2 Overview of the Mitochondrion and Dysfunction

1.2.1 Mitochondrial Structure

The mitochondrion is an organelle that regulates many essential functions, such as cellular respiration, calcium homeostasis, apoptosis, and heme synthesis (Protasoni and Zeviani, 2021). Its diverse range of regulation is still being discovered as recent studies have shown mitochondria regulating cell fate decisions and immune responses (Khacho *et al*., 2016; Matheoud *et al*., 2016). Mitochondria have two phospholipid bilayers, the OMM and the inner mitochondrial membrane (IMM), that divide the mitochondria in to two spaces, the intermembrane space and the matrix (Nunnari and Suomalainen, 2012; Protasoni and Zeviani, 2021). The OMM interacts with other subcellular components, such as the endoplasmic reticulum (ER), which is important for signaling between organelles (Hu *et al*., 2021). Invaginations in the IMM are called cristae and greatly increase the IMM's surface area, which is essential for energy production. The matrix is the location for many important reactions, such as the Kreb's cycle (Judge and Dodd, 2020). The matrix is also where mtDNA is stored; however, as this DNA only codes for 13 proteins, mitochondria still rely on nuclear DNA (Nunnari and Suomalainen, 2012).

1.2.2 Energy Production and the Electron Transport Chain

Perhaps the most well-known function of the mitochondria is its role in cellular respiration. The conversion of carbohydrates, fatty acids, and protein into energy has been extensively reviewed

by Judge and Dodd (2020), and thus for the purposes of this dissertation, we will only be overviewing the electron transport chain, the final step of aerobic metabolism.

The ETC consists of a group of complexes involved in a series of redox reactions to generate a proton gradient to power OXPHOS and generate adenosine triphosphate (ATP). The OXPHOS complexes are found within the cristae and pumps protons from the matrix to the intermembrane space (Protasoni and Zeviani, 2021; Zhao *et al*., 2019). To provide energy to the ETC, electron carriers, nicotinamide adenine dinucleotide (NADH) and flavin adenine dinucleotide ($FADH_2$), are reduced throughout the previous steps. NADH-CoQ oxidoreductase, complex I, facilitates the passing of the electrons from NADH to Coenzyme Q (CoQ) and pumps protons across the inner mitochondrial membrane (IMM). Succinyl-CoQ oxidoreductase, complex II, transfers of electrons from $FADH_2$ to CoQ. This complex is intimately integrated into the Krebs cycle and unlike complex I, the complex II does not pump protons across the IMM. Complex III, CoQ-cytochrome c oxidoreductase, transfers electrons from CoQ to cytochrome to pump protons. Complex IV, cytochrome c oxidase, allows the transfer of electrons to the final acceptor, oxygen, generating water as a by-product. The final protons are pumped here. The proton-motive gradient generated with flow back into the inner membrane space through complex V, F_1F_0ATP synthase, which uses the energy to catalyse oxidative level phosphorylation. For the ETC to function efficiently, complexes I, III, and IV arrange into a precise supercomplex (Guo *et al*., 2017). Other supercomplex combinations have been observed such as those between complexes I and III and complexes III and IV (Lobo-Jarne *et al*., 2020; Cogliati *et al*., 2016). Several proteins are also able to promote supercomplex assembly, such as cytochrome c oxidase subunit 7A-related protein (COX7RP) and the matrix-targeted isoform of myeloid cell leukaemia-1 (MCL1) (Cogliati *et al*., 2016; Perciavalle *et al*., 2012). As previously discussed, many PD models impair OXPHOS,

suggesting that maintaining efficiency may be a possible therapeutic approach (Bender *et al*., 2006; Pickrell *et al*., 2015; Reeve *et al*., 2013).

1.2.3 Mitochondrial Dynamics

Mitochondrial are dynamic organelles that can respond morphologically to the needs of the cell. For example, during autophagy, mitochondria elongate and maintain adequate levels of ATP production (Gomes *et al*., 2011). In contrast, during neural stem cell differentiation, mitochondria fragment to activate differentiation genes (Khacho *et al*., 2016). Mitochondrial dynamics have been shown to play a role in many other functions such as apoptosis, the cell stress response, and cell cycling (Wu *et al*., 2011; Mitra *et al*., 2009). Furthermore, abnormal mitochondrial dynamics has been associated with a variety of diseases, including PD (Züchner *et al*., 2004; Zanna *et al*., 2008; Carelli *et al*., 2015).

Mitochondrial fission is mediated by the dynamin-related GTPase, dynamin-related protein 1 (DRP) and OMM resident protein receptors (Smirnova *et al*., 2001). DRP1 is recruited to the OMM by these receptors and promotes complex formation to drive the constriction of the mitochondria (Korobova *et al*., 2013; Smirnova *et al*., 2001). Maintaining mitochondrial fission is important for mitochondrial quality control, as it allows for the removal of dysfunctional mitochondria (Han *et al*., 2020). Fusion of the OMM is mediated through the dynamin-related GTPases, Mitofusin 1 (MFN1) and Mitofusin 2 (MFN2), which are able to act cooperatively and independently (Chen *et al*., 2003). IMM fusion is regulated by the dynamin-related GTPase, Optic Atrophy 1 (OPA1) and other supporting factors (Song *et al*., 2007). Mitochondrial fusion is initiated when two mitochondria come into close contact, leading to MFN1 and 2 to tether the OMM together and allow them to fuse (Song *et al*., 2009). OPA1 is required for mediating IMM fusion, similarly to the OMM, through tethering and pulling the membranes together. OPA1 is

alternatively cleaved into long, membrane-bound and short, soluble isoforms, both of which were thought to be required for fusion; however, it has been shown that long OPA1 is sufficient for fusion (Song *et al*., 2009). While the role of short OPA1 is less clear, it may also be involved in maintaining normal cristae structure and respiration (Lee *et al*., 2017). Other than fusion, OPA1 is also important for cristae remodeling and tightening, giving rise to more ETC proteins and supercomplexes, leading to increased OXPHOS (Cogliati *et al*., 2013; Patten *et al*., 2014). Interestingly, regulation of cristae structure can be independent of IMM fusion. Inhibition IMM fusion without disrupting OPA1 did not alter cristae shape, but OPA1 knockdown resulted in widened, aberrant cristae (Frezza *et al*., 2006). Furthermore, OPA1 has been shown to be essential for mitophagy regulation, and apoptotic signaling (Glytsou *et al*., 2016; Liao *et al*., 2017).

1.2.4 OPA1 Mutations and Parkinsonism

OPA1 deficits have been used as a model to investigate the role of mitochondrial dysfunction in PD (Iannielli *et al*., 2018; Iannielli *et al*., 2019). Not only does *in vitro* OPA1-deficient models exhibit key cellular defects of PD, such as ROS production and reduced OXPHOS efficiencies, but certain patients with OPA1 mutations also develop parkinsonism (Iannielli *et al*., 2018; Carelli *et al*., 2015). A subset of patients who suffer from dominant optic atrophy have OPA1 mutations, leading to progressive visual failure due to optic nerve degeneration (Liao *et al*., 2017); however, these patients may also develop further neurological phenotypes (Zanna *et al*., 2008). OPA1 mutations have been shown to be partially responsible for the accumulation of mtDNA deletions and may play a role mtDNA maintenance (Carelli *et al*., 2015; Amati-Bonneau *et al*., 2008). In fibroblasts derived from dominant optic atrophy, OXPHOS and mitochondrial structure was affected (Zanna *et al*., 2008). Furthermore, patients with OPA1 missense mutations develop parkinsonism and dementia, suggesting that OPA1-mutant neurons can be a viable PD

model (Carelli *et al*., 2015). In induced pluripotent stem cell-derived neurons from OPA1-mutant patients showed a reduced number of active synapses, decreased cell viability, reduced OXPHOS, and increased oxidative stress (Iannielli *et al*., 2019; Iannielli *et al*., 2018). These data suggest that impairment of mitochondrial fusion in neurons through OPA1 can be suitable for investigating the role of mitochondrial dysfunction in PD.

1.2.5 Mitochondrial ROS Production

During the energy production process, electrons can leak from the ETC and produce ROS (Zhao *et al*., 2019). ROS is a broad term that describes oxygen derived free radicals, which is mainly generated at complexes I and III (Mailloux *et al*., 2013). ROS is an important second messenger that can regulate functions such as hypoxia, differentiation, activation of the innate immune system, and mitochondrial metabolism (Mailloux *et al*., 2013; Khacho *et al*., 2016; Nakahira *et al*., 2011); however, ROS can be damaging to the cell, leading to oxidative damage to mtDNA, lipid peroxidation, and cell death (Circu *et al*., 2009; Mailloux *et al*., 2013). As mentioned previously, dysregulated levels of ROS have been associated with the development of PD, damaging mtDNA and inducing cell death (Grünewald *et al*., 2019; Inden *et al*., 2011; Kang *et al*., 2009). To prevent buildup of ROS, the cell uses multiple antioxidant systems to metabolize free radicals (Sinha *et al*., 2013). Furthermore, antioxidant molecules have also been used to bolster the antioxidant response (Khacho *et al*., 2016; Tardiolo *et al*., 2018). Many studies have shown a protective effect of ROS reduction in PD models (Jin Jung *et al*., 2021; Pacifici *et al*., 2022; Chen *et al*., 2018). As mentioned previously, due to their intrinsic high basal energy requirements, DA neurons in the SN naturally produce more ROS which may partially explain their vulnerability to environmental and genetic insults (Pacelli *et al*., 2015).

1.3 The Integrated Stress Response

1.3.1 Overview of the Integrated Stress Response

The integrated stress response (ISR) is a signaling pathway which responds to a variety of cell stressors including amino acid and glucose deprivation, virus infection, ER stress, hypoxia, and oxidative stress (Pakos-Zebrucka *et al*., 2016) (**Fig 2**). These stressors lead to the phosphorylation of the 2A subunit of eukaryotic translation initiation factor (eIF2α) by eIF2α kinases. There are four eIF2α kinases: double-stranded RNA-dependent protein kinase (PKR), PKR-like ER kinase (PERK), heme-regulated eIF2α kinase (HRI), and general control non-derepressible 2 (GCN2). Each can respond to distinct stressors with some functional overlap between them. For example, PERK responses to ROS-induced ER stress, PKR activates in response to viral infection, and GCN2 is activated in response to amino acid deprivation (Amodio *et al*., 2019; Verfaillie *et al*., 2012; Lemaire *et al*., 2008, Longchamp *et al*., 2018). The eIF2α kinases are activated by self-dimerization and autophosphorylation. They converge on the phosphorylation of eIF2α, resulting in a global decrease in protein translation while upregulating certain genes to resolve the stress. Activating transcription factor 4 (ATF4) is an important effector for the ISR. By upregulating and dimerizing with a wide variety of downstream targets, ATF4 can regulate a wide range of functions depending on the cellular needs. Many of ATF4's downstream targets are homeostatic genes; however, if the stress is too severe or prolonged, ATF4 binds to other factors to promote apoptosis (Bai *et al*., 2021; Aimé *et al*., 2020, Demmings *et al*., 2021). For example, under oxidative stress ATF4 can upregulate solute carrier family 7 member 11 (Slc7a11), a cysteine transporter, to promote glutathione biosynthesis and resolve the stress (Bai *et al*., 2021). On the other hand, ATF4 has been shown to induce and bind to C/EBP homologous protein (Chop) to induce apoptosis via p53 upregulated modulator of apoptosis (PUMA) (Galehdar

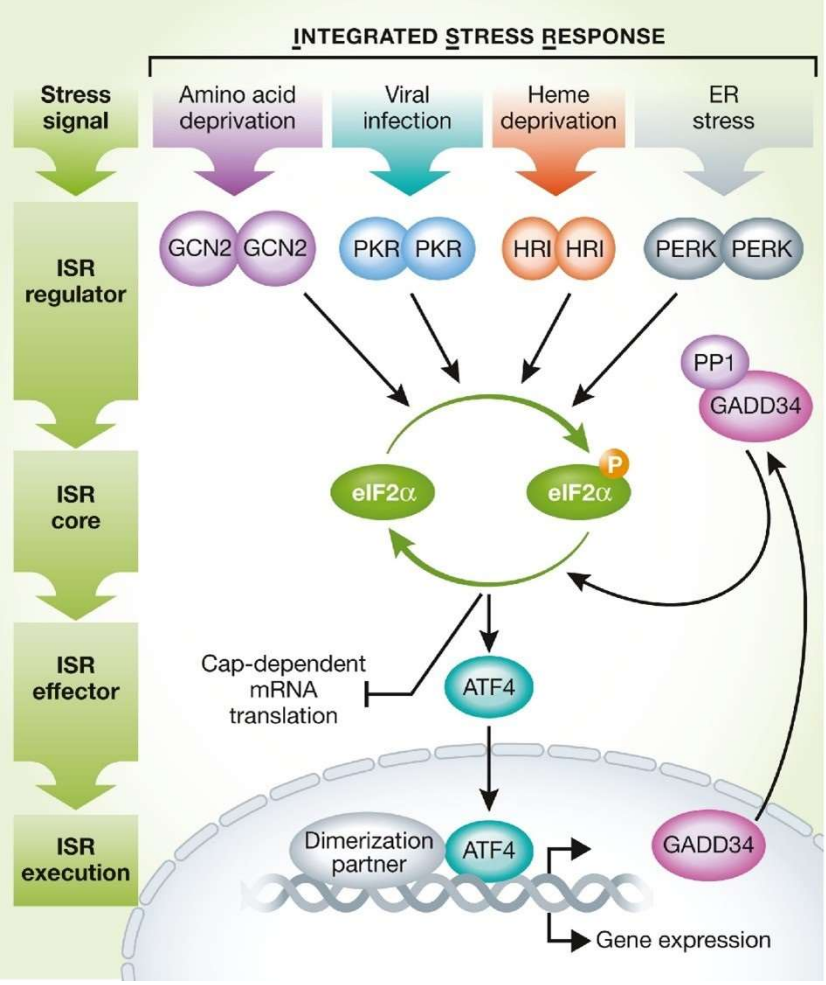

Fig 2. The ISR is activated by multiple stressors to maintain homeostasis. A diverse range of stressors activate eIF2α kinases, HRI, GCN2, PKR, and PERK, which converge on the phosphorylation of eIF2α. Global translation is decreased while preferentially translating ISR-specific genes such as ATF4. Initially, ATF4 will upregulate genes involved in maintaining homeostasis, but may switch to a pro-death role if the stress is unresolved. The ISR is terminated by the dephosphorylation of eIF2α by GADD34. Adapted from Pakos-Zebrucka *et al*. (2016).

et al., 2010). If the stress is resolved, the ISR is terminated by the phosphatase, growth arrest and DNA damage-inducible protein (GADD34), which dephosphorylates eIF2α to restore protein translation (Kojima *et al*., 2003).

1.3.2 The ISR and ATF4 in PD

While the ISR and ATF4 have been shown to be upregulated in cellular, animal, and post-mortem models of PD, their role is still unclear. Certain studies have reported that ATF4 is protective in cellular PD models (Sun *et al*., 2013; Sun *et al*., 2018; Inoue *et al*., 2018); however, numerous studies have also implicated ATF4-induced cell death as a critical player in PD progression. In a cellular PD model, induced by MPTP or 6-OHDA treatment, ATF4 was upregulated along with its pro-apoptotic downstream targets, Chop, Tribbles homologue 3 (Trib3), and Puma (Demmings *et al*., 2021). Furthermore, neurons cultured from ATF4 knockout mice showed less cell death after drug treatment compared to wild type. Interestingly, Adaptaquin, a prolyl hydrolase inhibitor was shown to be protective in both cellular and animal models, by inhibiting ATF4 in an eIF2α-independent manner (Aimé *et al*., 2020). The presence of unfolded proteins and protein aggregates, which have been seen in PD, can lead to ER stress and activation of the ISR (Galehdar *et al*., 2010). Neurons treated with the ER stressors, tunicamycin and thapsigargin, induced cell death through the upregulation of ATF4, and its downstream target, Chop and Puma. Neurons from ATF4 knockout mice showed attenuated cell death and reduced Chop and Puma activation. Injection of α-Syn-expressing adeno-associated virus (AAV) into rat SN showed an increase in ATF4 expression and a subsequent loss of dopaminergic neurons (Gully *et al*., 2016). Furthermore, injecting with an ATF4-expressing AAV produced a similar effect, resulting in a decrease in dopaminergic neurons and an increase in caspase activity. Activation of the ISR has also been found in the midbrain, hippocampus, and cortex of post-mortem PD brain

tissue (Mercado *et al*., 2018). Interestingly, certain patients had increased αSYN, phosphorylated PERK, and phosphorylated eIF2α expression without displaying any clinical symptoms, suggesting that ISR activation may occur very early during PD. While the dual actions of ATF4 are complex, this suggests its downstream effects depend on the extent of the stress as well as the cellular context.

1.3.3 The Intrinsic Apoptosis Signaling Pathway

Apoptosis, programmed cell death, is a mechanism require for normal development as well as a response to cell stress and damage (Protasoni and Zeviani, 2021). Cells undergoing apoptosis morphologically show, shrinking cell size, blebbing of the cell membrane, phosphatidylserine exposure, and condensed, fragmented nuclei (Elmore, 2007; Sinha *et al*., 2013). Apoptosis can occur by extrinsic pathway or a mitochondria-regulated intrinsic pathway, both of which have been extensively reviewed by Elmore (2007). Other than apoptosis, other forms of cell death such as ferroptosis and necrosis have been implicated in PD (Kim *et al*., 2005; Do Van *et al*., 2016; Callizot *et al*., 2019); however, for the purposes of this dissertation, we will be overviewing the intrinsic apoptotic pathway, which acts through a caspase cascade. Caspases are typically present in a proenzyme form and must be cleaved to initiate the cell death process, allowing for rapid cell death. Caspases can be organized into initiators, which include caspases-2, -8, -9, -10, and executioners, caspases-3, -6, -7 (Elmore, 2007). The initiators cleave the proenzyme executioners, which go on to cleave other cellular substrates to cause the hallmark apoptotic morphology (Van Opdenbosch and Lamkanfi, 2019). Multiple stimuli such as radiation, hypoxia, ROS, toxin, and viral infection, are able to trigger the intrinsic pathway. The proapoptotic proteins, BAX and BAK, oligomerize and form a mitochondrial permeability transition pore (PTP) on the OMM, leading to the release of pro-apoptotic proteins. Cytochrome c, previously mentioned to be an electron carrier of the ETC,

binds to apoptotic peptidase activating factor 1 (Apaf1) and to form an apoptosome and activates caspase-9 (Elmore, 2007). Smac/DIABLO and HtrA2/Omi promote cell death by inhibiting inhibitors of apoptosis proteins (IAP). Finally, apoptosis inducing factor (AIF), Endonuclease G, and caspase-activated DNAse (CAD) are translocated to the nucleus to induce DNA fragmentations. CAD in particular is cleaved by caspase-3 and promotes advanced chromatin condensation while endonuclease G and AIF are caspase independent. Regulation of the mitochondrial apoptotic events are tightly regulated by B-cell lymphoma 2 (BCL2) family proteins.

1.4 MCL1

1.4.1 The BCL2 Family Regulates Apoptosis

The BCL2 family has long been known for their regulation of apoptosis. All members contain the BCL2 homology domain and can be divided into anti-apoptotic and pro-apoptotic (Letai *et al*., 2002). Amongst the pro-apoptotic, BAX and BAK are special, as they form mitochondrial PTP. The rest of the pro- and anti-apoptotic BCL2 family members are in constant competition to influence the formation of the mitochondrial PTP, which is influenced by a variety of damage signals (Certo *et al*., 2006). A subset of pro-apoptotic BCL2 proteins, such as BID, BIM, and PUMA, directly induce BAX/BAK oligomerization, leading to mitochondrial PTP formation (Letai *et al*., 2002; Cartron *et al*., 2004; Kuwana *et al*., 2005). Anti-apoptotic proteins, which include BCL2, BCL-X_L, BCL-w, and MCL1, can bind to pro-apoptotic BCL2 family members to prevent their interaction with BAX/BAK, or directly binding to BAX/BAK (Kuwana *et* al., 2005). The other subset of pro-apoptotic BCL2 proteins, such as BAD, Noxa, and BIK,

promote cell death by sequestering the anti-apoptotic proteins, allowing for BAX and BAK oligomerization (Letai *et al*., 2002; Lopez *et al*., 2010).

1.4.2 MCL1 and its Isoforms

MCL1 was first identified as a protein induced in human myeloblastic leukemia (Sancho *et al*., 2021). MCL1, an anti-apoptotic BCL2 family protein, has been shown to play an important role in development of neurons, lymphocytes, and neutrophils, and regulates autophagy (Arbour *et al*., 2008; Fogarty *et al*., 2019; Dzhagalov *et al*., 2008; Steimer *et al*., 2009; Germain *et al*., 2011). Interestingly, MCL1 appears to play an important role in the development and survival of DA neurons (Robinson *et al*., 2018). MCL1 undergoes alternative cleavage at the N-terminus, possibly by the matrix processing peptidase, generating different isoforms (Perciavalle *et al*., 2012; Huang and Yang-Yen, 2010). These different isoforms are targeted to different areas of the mitochondria and have distinct functions (**Fig 3**). The OMM-targeted form (MCL1-OM) demonstrates the traditional anti-apoptotic BCL2 family function, blocking apoptosis presumably by sequestering and preventing the translocation of BAK and BAX to the OMM (Willis *et al*., 2005; Chen *et al*., 2005). The matrix-targeted form (MCL1-Matrix), however, has been shown to have distinct functions which have been demonstrated to be essential for proper mitochondrial function (Perciavalle *et al*., 2012).

1.4.3 MCL1-Matrix's Role in Maintaining Mitochondrial Function

MCL1-Matrix has been demonstrated to regulate cristae structure, fusion, and OXPHOS (Perciavalle *et al*., 2012). The deletion of MCL1 in mouse embryonic fibroblasts resulted in swollen, disorganized cristae and impaired fusion, which could be rescued with wildtype MCL1 or MCL1-Matrix, but not MCL-OM. This cristae disruption was also associated with impairment

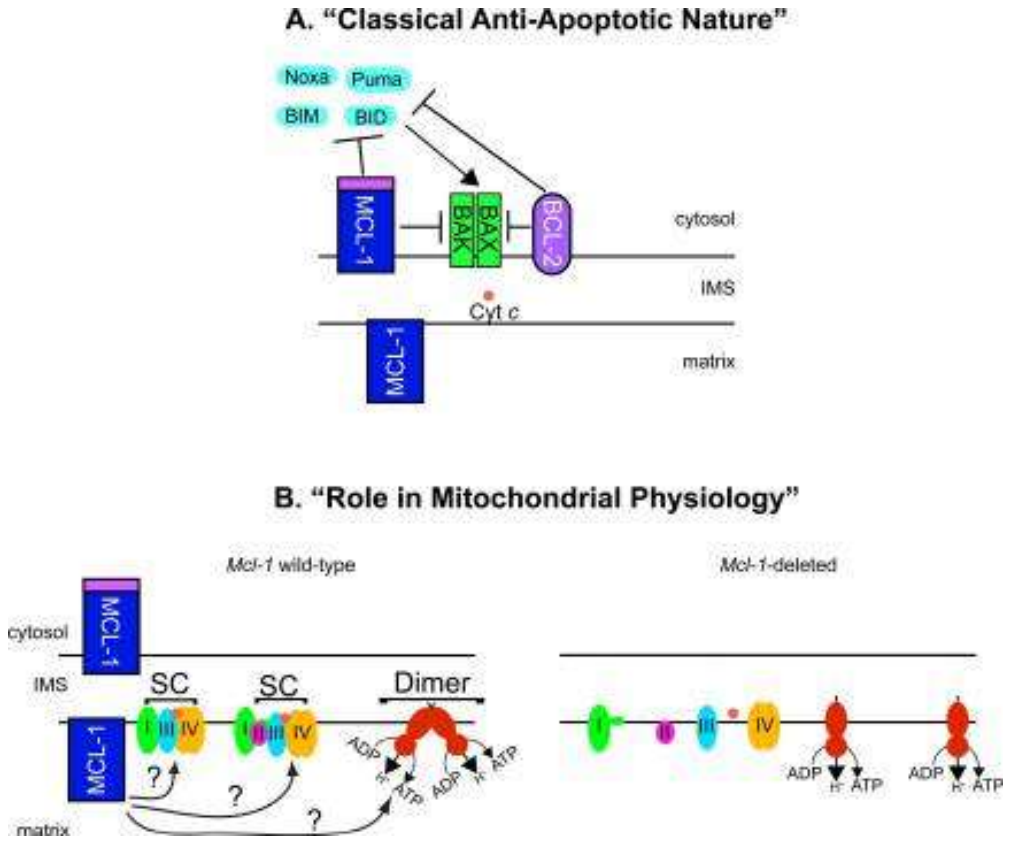

Fig 3. MCL1 is alternatively cleaved and translocated. MCL1 has two identified isoforms that are translocated to different regions of the mitochondria. MCL1-OM functions as a traditional anti-apoptotic BCL2 protein and sequesters BAX/BAK. MCL1-Matrix localizes to the inner mitochondrial membrane where it regulates respiration through supercomplex assembly. From Perciavalle and Opferman, (2013).

with the ETC due to alterations in supercomplexes assembly, particularity those containing complexes I, III, and IV. Furthermore, F_1F_0ATP synthase oligomerization was reduced along with ATP production. In MCL1 deficient fibroblasts, respiration was decreased but could be rescued with wildtype MCL1 or MCL1-Matrix, but not MCL-OM, further emphasizing the important role of the matrix isoform in mitochondrial function. Recently, our lab has shown that manipulating mitochondrial integrity through MCL1-Matrix can maintain mitochondrial function and prevent cell death under acute mitochondrial stress (Anilkumar *et al*., 2020). Under acute NDMA treatment and oxygen/glucose deprivation, both MCL-Matrix and -OM, prevented cell death; however, these appeared to be done through different mechanisms. Where MCL1-OM predominantly acts in a traditional anti-apoptotic BCL2 manner, MCL1-Matrix was shown to prevent cell death by blocking the formation of the mitochondrial PTP through interactions with complex V. In both NMDA-induced stress and oxygen/glucose deprivation, MCL-Matrix was effective in maintaining respiration and ATP production similar to a sham treatment. Under the excitotoxic stress, MCL1-Matrix infected neurons maintained mitochondrial membrane potential compared to the control and OM infected neurons. In MCl1 deficient mouse embryonic fibroblasts, MCL1-Matrix infected neurons showed improved Ca^{2+} retention suggesting that Matrix increases the maximal capacity to delay mitochondrial PTP opening. Furthermore, in parkin knockout DA neurons, MCL1-Matrix promoted survival, demonstrated by an increase in number at day 11 in culture, compared to an mCherry control. These data suggest that MCL1-Matrix, through mitochondrial reconfiguration, provides a broad protective effect which may lead the way for the development of neuroprotective treatments.

1.5 Rational and Hypothesis

There is now compelling evidence that mitochondrial dysfunction is a key player in PD progression. The goal of this thesis is to determine if enhancing mitochondrial integrity may be a strategy to prevent neurodegeneration in PD. First, to identify key stress pathways involved, we used a mitochondrial dysfunction model to investigate pathways which are activated and its subsequent downstream effects as a readout for neuronal stress and impairment. Next, we determined if manipulating mitochondrial integrity and efficiency, using MCL1-Matrix which can function as a supercomplex assembly factor, will reduce the activation of these stressors and promote neuronal survival. We induced mitochondrial dysfunction by knocking down OPA1 in embryonic neurons, an *in vitro* model that exhibits key hallmarks of PD, to characterize and rescue deficits. **We hypothesize that mitochondrial dysfunction induces stress pathways which is a key mechanism in neuronal impairment. By manipulating mitochondrial integrity through the manipulation of MCL1 isoforms, -OM and -Matrix, we will reduce neuronal deficits in PD models.** To test this hypothesis, there are two aims:

Aim 1: Characterizing changes in a mitochondrial dysfunction model.

Aim 2: Manipulating mitochondrial integrity to rescue neuronal impairment under stress.

MATERIALS AND METHODS

2.1 Human Embryonic Kidney 293T (HEK293T) Culture

HEK293T cells were purchased from American Type Culture Collection (ATCC; CRL-3216). HEK293T cells were grown in Dulbecco's modified Eagle's medium (DMEM) supplemented with 10% fetal bovine serum (FBS) and 100 Units/mL of Penicillin/Streptomycin. HEK293T cells were cultured at 37°C with 5% carbon dioxide (CO_2) in a humidified incubator and passaged at 80% confluency.

2.2 Recombinant Lentivirus Production

Lentivirus packaging plasmids, pMd2.g (Addgene; 12259) and psPax2 (Addgene; 12260) were provided by Dr. Didier Trono through Addgene. The pWPXLd-GFP, -MCL1-OM, and -MCL1-Matrix plasmids were generated as described in Perciavalle *et al*. (2012) and Anilkumar *et al*. (2020). In brief, MCL1-OM was developed by replacing arginine 5 and 6 with alanine of mouse MCL1 cDNA. MCL1-Matrix was developed by deleting 67 amino-terminal amino acids by and fusing 50 amino acids of *Neurospora crassa* ATP-synthase to the amino terminal using polymerase chain reaction (PCR). These constructs were inserted into the pWPLXd lentivirus expression plasmid (Addgene; 12258). shRNA scramble control (5'-CAACAAGATGAAGAGCACCAA-3') and mouse specific shRNA to OPA1 (5'-GCCTGACTTTATATGGGAAAT-3') were inserted into the pLKO.1-TRC backbone (Addgene; 10878) as previously described in Khacho *et al*. (2014).

Lentiviruses were generated in HEK293T cells by polyethyleneimine (PEI) co-transfection of the packaging plasmids and the gene of interest plasmids. Plasmids used are reported in **Table 1**. Media was changed 16 hours post-transfection, and virus-containing media was collected 40- and 56-hours post-transfection. Virus-containing media was filtered through a 0.45 μm

Plasmid	Gene of Interest	Source
pMD2.G	VSV-G envelope	Addgene; 11259
psPAX2	2nd generation lentiviral packaging plasmid	Addgene; 12260
pLKO-shOPA1	Short hairpin targeting OPA1	Khacho *et al*., 2016
pLKO-shCtrl	Short hairpin scramble control	Khacho *et al*., 2016
pWPXLd-GFP	GFP	Anilkumar *et al*., 2020
pWPXLd-MCL1-OM	MCL1-OM	Perciavalle *et al*., 2012 Anilkumar *et al*., 2020
pWPXLd-MCL1-OM	MCL1-Matrix	Perciavlle *et al*., 2012 Anilkumar *et al*., 2020

Table 1: List of plasmids used for Lentivirus preparation

Polyvinylidene Fluoride (PVDF) filter, then concentrated by centrifugation at 68,300 g for 2 hours at 4°C. Virus was resuspended in phosphate buffered saline (PBS) and stored at -80°C until use. Virus was titred using the QuickTitre Lentivirus titre kit (Cell Biolabs; VPK-107) as per manufacturer's instructions. Titre is expressed in transduction units (TU) per mL.

2.3 Primary Embryonic Neuron Culture

All experimental protocols involving mice were approved by the University of Ottawa Animal Care Committee. Embryos aged E13-14 from pregnant CD1 genetic background mice (Charles River Laboratories; Montreal, QC) were extracted. Cortices were extracted by removing the olfactory bulbs, cerebellum, and meninges. To dissociate into single cells, tissues was chemically digested with trypsin and mechanically digested using flame-polished pasteur pipette. Neurons were cultured at 37°C with 5% CO_2 in a humidified incubator in neurobasal media containing 1X B27; 1X N2; 100 Units/mL Penicillin/Streptomycin, and 0.6 mM L-glutamine. Full media change was performed upon day 3 *in vitro* and half media change every subsequent third day. For shOPA1 experiments, neurons were treated with 6 MOI (multiplicity of infection) of OPA1 knockdown lentivirus (shOPA1) or a scrambled control (shCtrl) on day 6 *in vitro*. For MCL1 experiments, neurons were treated with 5 MOI of MCL1-OM, MCL-Matrix, or a GFP control on the day of seeding. For rotenone experiments, neurons were treated with 15, 25, 30 nM of rotenone, or a vehicle containing dimethyl sulfoxide (DMSO) on day 6 *in vitro* for 6, 12, or 24 hours.

2.4 Western Blot

To extract protein, cells were washed once with cold PBS, radioimmunoprecipitation assay (RIPA) buffer (containing 400 μM sodium orthovanadate, 1 mM DTT, and 1X protease inhibitor

cocktail [Sigma; P8340]) was added, and cells were scraped. Cells were titrated with a pipette to lyse and centrifuged at 16,200 g for 15 min. Protein-containing supernatant was taken and protein was quantified using the BioRad DC protein assay (BioRad; 5000116) as per manufacture's instructions. Protein was diluted in RIPA buffer and 1X Laemmli's buffer with 2% β-mercaptoethanol and boiled for 5 min. Proteins were run on an SDS-Page gel and transferred to a PVDF membrane. Membranes were blocked in 5% skim milk in tris-buffered saline with Tween 20 (TBST) for one hour at room temperature. Membranes were incubated in primary antibody overnight at 4°C. A list of antibodies used are found in **Table 2**. Membranes were washed for 7 minutes 3x in 1X TBST before incubation with the appropriate 1:10,000 secondary antibody. Membranes were washed for 15 minutes for 3x in 1X TBST. Blots were incubated in Clarity Western ECL Substrate (BioRad; 170-5061) for 5 mins and imaged. Densitometry analysis was done using Fiji (ImageJ) software and normalized to β-actin control.

2.5 Quantitative Real Time PCR

To extract RNA, TRIzol Reagent was added, and cells were scraped. Cells were incubated with chloroform, then centrifuged to separate the aqueous phase. The aqueous phase was taken, and glycogen was added. The aqueous phase was incubated with isopropanol to precipitate the RNA, and centrifuged. The isopropanol was removed, washed twice with 75% ethanol, and air dried for 10 minutes. The RNA pellet was resuspended in sterile water containing 0.1 mM of ethylenediaminetetraacetic acid (EDTA) and incubated at 55°C for 10 minutes. The RNA was treated with DNase using the RNase-free DNase set (Qiagen; 79254) as per manufacturer's instructions. 250 ng of RNA was converted to cDNA using the SupersScript IV VILO Master Mix

Primary Antibody	Host Species	Manufacturer	Dilution
Opa1	Rabbit	Abcam; ab42364	1:3000
Atf4	Rabbit	Cell Signaling Technology; 11815	1:1000
Mcl1	Rabbit	Rockland; 600-401-394	1:5000
Snap25	Mouse	Santa Cruz Biotechnology; sc-20038	1:1000
Total Oxphos Cocktail	Mouse	Abcam; ab110413	1:1000
β-Actin	Mouse	Santa Cruz Biotechnology; sc-8432	1:10,000
Secondary Antibody		**Manufacturer**	**Dilution**
Anti-Rabbit HRP	Goat	Promega; W4011	1:10,000
Anti-Mouse HRP	Goat	Promega; W402B	1:10,000

Table 2: List of primary and secondary antibodies used for immunoblotting.

(Invitrogen; 11756050) as per manufacturer's instructions. Converted cDNA was diluted to 1 ng/µL in 10 mM Tris-HCl.

Gene expression was quantified using the HostStarTaq DNA polymerase (Qiagen; 203205) as per manufacturer's instructions. The cDNA was amplified using the BioRad CFX96 Real-Time PCR system (BioRad; 3600037) using the following protocol: 95°C for 15 min, 94°C to 60°C to 72°C for 15 sec each cycled 45 times, 95°C for 1 min, 60°C for 30 sec, then 95°C for 1 min. A list of primers used are found in **Table 3**. Relative gene expression was analysed using the $2^{-\Delta\Delta CT}$ method (Livak and Schmittgen, 2001) and normalized to Gapdh control.

2.6 Cell Viability Assay

To analyse cell viability under rotenone treatment, neurons were plated at 2e6 cells/well in 6-well plates cultured in phenol red free media. After rotenone treatment, 100 uL of CellTitre 6 AQ_{ueous} One Solution (MTS) (Promega; G3580) was added to each well an incubated for 1 hour. Colorimetric intensity was read at 490 nm (690 nm reference). Each control condition was set to 100% viability, and no-cell blank was set as 0%. The cell viability was calculated as follows:

$$\%\,\text{Viability} = \frac{A_{490} - A_{690}}{A_{Control}} \times 100\%$$

2.7 MitoSOX Assay

Cells were treated with 1 µg/mL of Hoechst 33342 for 15 min, then media was replaced with phenol red-free neurobasal media. Cells were kept on ice before imaging. Media was removed and 5 µM of MitoSOX red (ThermoFisher Scientific; M36008) diluted in PBS was added to the cells. Cells were incubated for 5 minutes on a heated stage and imaged using the DeltaVision Elite

RT-qPCR Primer	Forward Sequence (5' to 3')	Reverse Sequence (5' to 3')
Opa1	TGG AAT ACA AAG AAA CGT ACC GC	GGG CAG GAT GAT GTG AAC GA
Atf4	AAA AGG CAT CCT CCT TGC G	CTT GAT GTC CCC CTT CGA CC
Chop	ACA GAG GTC ACA GCG ACA TC	GGG CAC TGA CCA CTC TGT TT
E2f1	CTG CAG CAA CTG CAG GAG AG	CTC CGA AAG CAG TTG CAG CTG
Chac1	TGG TGA CCC TCC TTG AAG AC	TTG GTC AGG GGT GTC TTG AG
Slc7a11	GTC TGC CTG TGG AGT ACT GT	ATT ACG AGC AGT TCC ACC CA
Snap47	TGC CAT TGC GTC TTC TGC G	AGG AAC AAG ACC AGG AGT GGA C
Syt9	ATC TAC CAC CTG CGG GAC C	AGA CCA CAG GCA GTA ACC ACG
Gapdh	GGT GAA GGT CGG TGT GAA CG	CTC GCT CCT GGA AGA TGG TG

Table 3: List of primers used for RT-qPCR.

microscope. Arbitrary fluorescence intensity was determined by quantifying the MitoSOX red intensity that overlaps with Hoechst 33342 and normalized to average control intensity.

2.8 Statistical Analysis

Analysis was performed with GraphPad Prism 8 (GraphPad Inc, LaJolla, CA). The shOPA1 western blots and qPCRs were analysed with a two-way t-test. Cell viability assays were analysed with a two-way analysis of variance (ANOVA), followed by Tukey's post-hoc test. The MCL1 western blots and MitoSOX assay were analysed with a two-way ANOVA followed by a Tukey's post-hoc test.

RESULTS

3.1 OPA1 knockdown leads to the upregulation of Atf4 and its downstream targets

We first asked what pathways are activated during mitochondrial dysfunction in neurons. An RNA bulk sequencing was previously performed on neurons treated with shOPA1 or shCtrl on the day of seeding and harvested 4 days *in vitro* (DIV). Of note, *Atf4* transcripts were found to be significantly upregulated in shOPA1, along with a downstream target, *Redd1* (Bilen and Fong, unpublished) (**Fig 4a**). Thus, to investigate the stress pathways activated from mitochondrial dysfunction in post-mitotic neurons, we knocked down Opa1 with lentivirus expressing short hairpin RNA (shRNA). As described previously, OPA1 deficiencies have been associated with OXPHOS dysfunction and parkinsonism development (Iannielli *et al*., 2018; Zanna *et al*., 2008). Through immunoblot, we show that Opa1 is significantly decreased by ~86.8% by shOPA1 treatment compared to control (**Fig 4b, c**). Furthermore, Opa1 knockdown in neurons lead to an ~88.9% significant decrease in complex I expression, resembling neurotoxin models of rotenone and MPP^+ (**Fig 4b**, **c**; Inden *et al*., 2011). To validate the RNA bulk sequencing results, Atf4 protein expression was quantified in post-mitotic neurons treated with shOPA1 and was found to be significantly upregulated compared to shCtrl by ~24.9 fold (**Fig 4d**, **e**). Furthermore, Atf4 and its downstream targets, *Chop*, *Slc7a11*, and *Chac1*, showed significantly increased gene expression, suggesting that the ISR was activated (**Fig 4f**; Bilen, unpublished). Other pathways may also be induced such as the oxidative stress response, from increased *Chac1* and *Slc7a11* (**Fig 4f**). These data suggest that mitochondrial dysfunction leads to the activation of the ISR.

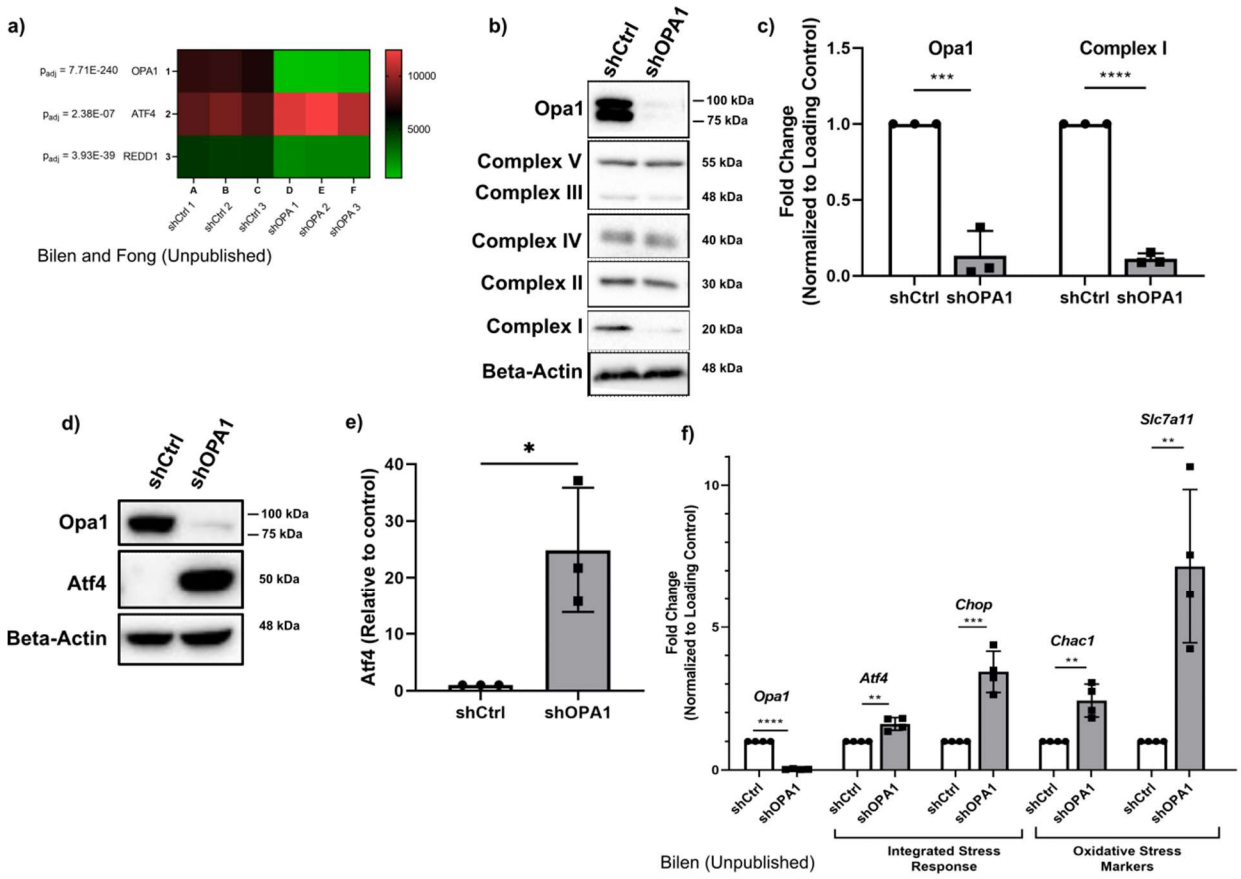

Fig 4. OPA1 knockdown induces ATF4 upregulation and stress markers a) Embryonic neurons (E12-E13) were infected with shCtrl or shOPA1 lentivirus DIV0 and mRNA was harvested DIV4. mRNA was sequenced and number of reads were plotted. Data suggests an upregulation of Atf4 following Opa1 knockdown **b)** Post-mitotic neurons were infected with 6 MOI of shOPA1 DIV 6 and harvested DIV 12. Data suggests a decrease in Complex I **c)** Quantification of Opa1 and Complex I. Data shown are mean fold change (N=3) ± SD. **d)** Post-mitotic neurons infected with shOPA1 and harvested DIV11. Data suggests an increase in ATF4 following OPA1 knockdown. **e)** Quantification of Opa1 and Atf4. Data shown are mean fold change (N=3) ± SD. **f)** Quantification of *Opa1*; integrated stress response (*Atf4, Chop*); and oxidative stress marker (*Chac1, Slc7a11*) gene expression. Data suggests an increase in Atf4 and its downstream targets. Data shown are mean fold change (N=4) ± SD. All data was analysed with two-tailed unpaired t-test. * p<0.05, ** p<0.01, *** p<0.001, **** p<0.0001

3.2 OPA1 knockdown leads to down regulation of synaptic genes

Next, we wanted to ask if mitochondrial dysfunction leads to neuronal impairment. To examine the expression of synaptic proteins after shOPA1 knockdown, the RNA bulk sequencing was analysed and potential deficits and functions were determined with gene ontology (**Fig 5a**; Bilen and Fong, unpublished). Of note, many synaptic genes involved in signaling between neurons, such as vesicle fusion and neurotransmitter transport, was found to be affected. Furthermore, it was found that multiple synaptic markers are altered in PD models, and are associated with cognitive decline, suggest that synaptic gene expression can be used as a readout of neuronal function (Berezcki *et al*., 2016; Berezcki *et al*., 2018). In particular, protein regulating calcium ion (Ca^{2+}) sensing, such as the synaptotagmins (SYT), and synaptic vesicle exocytosis, such as the Synaptosomal-associated proteins (SNAP) have been shown to be impaired (Bereczki *et al*., 2018; Krebs *et al*., 2013). We quantified the protein expression of Snap25, an essential factor of the SNARE complex involved in synaptic vesicle exocytosis and found it was significantly lower by ~37.0% in shOPA1-treated post-mitotic neurons compared to control (**Fig b**, **c**). Similarity, the gene expression of *Snap47*, another component of the SNARE complex, and *Syt9*, a Ca^{2+} sensor involved in exocytosis, was also shown to be significantly decreased by ~70.5% and ~77.3% respectively (**Fig 5d**). These data suggest that mitochondrial dysfunction is associated with neuronal impairment.

3.3 MCL1-OM and -Matrix prevent rotenone-induced cell death

As cell death is a major component in PD progression, we wanted to ask if manipulating mitochondrial integrity with MCL1-Matrix protects from mitochondrial dysfunction-associated cell death. Rotenone, a complex I inhibitor, has been used as PD model and causes apoptosis in a

a)

Downregulated		Log2 Fold Change
Snap47	synaptosomal-associated protein, 47	-1.48
Syt9	synaptotagmin IX	-1.29
Sv2b	synaptic vesicle glycoprotein 2 b	-0.96
Esyt1	extended synaptotagmin-like protein 1	-1.11
Snap25	synaptosomal-associated protein 25	-0.57
Snap91	synaptosomal-associated protein 91	-0.73
Syt14	synaptotagmin XIV	-0.64
Llph	LLP homolog, long-term synaptic facilitation (Aplysia)	-0.66
Syt13	synaptotagmin XIII	-0.74
Sv2c	synaptic vesicle glycoprotein 2c	-0.66
Synpo	synaptopodin	-0.70
Esyt3	extended synaptotagmin-like protein 3	-0.72

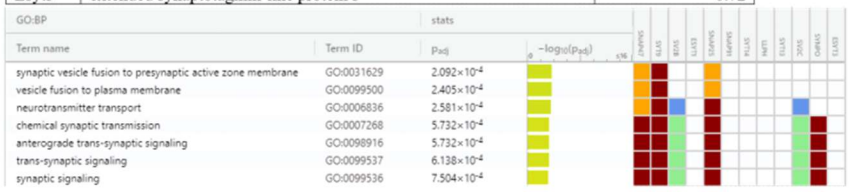

Upregulated		Log2 Fold Change
Syp	synaptophysin	1.31
Syt12	synaptotagmin XII	1.81
Syn2	synapsin II	0.57
Syap1	synapse associated protein 1	0.50
Syce2	synaptonemal complex central element protein 2	0.87
Rims1	regulating synaptic membrane exocytosis 1	0.52
Sycp2	synaptonemal complex protein 2	0.70

Bilen and Fong (Unpublished)

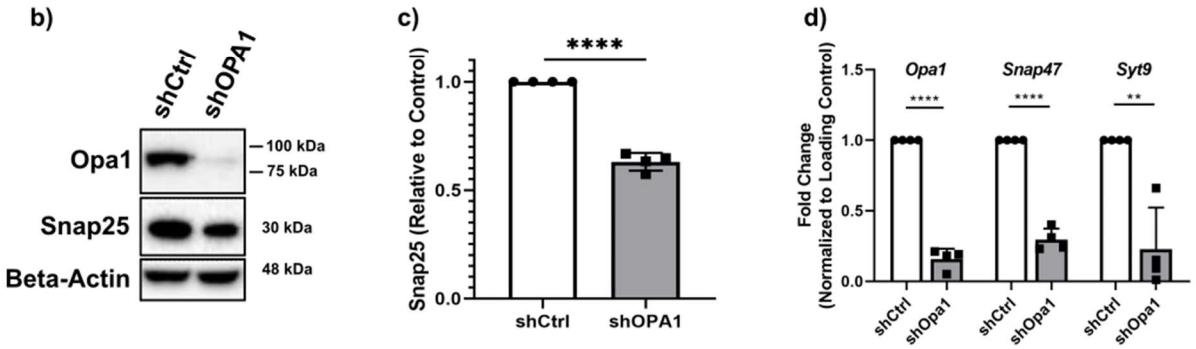

Fig 5. OPA1 knockdown leads to downregulation of synaptic genes a) Embryonic neurons (E12-E13) were infected with shOPA1 or shCtrl and RNA was extracted 4 days after for RNA bulk-seq. Significantly downregulated and upregulated synaptic-related proteins with fold change > 0.5 were selected and run through g:Profiler to determine biological processes. Relevant biological processes were selected for $P_{adj} < 10^{-4}$. Post-mitotic neurons were infected with 6 MOI of shOPA1 DIV6 and harvested DIV12. **b)** Western blot analysis of Snap25 suggesting a decrease in protein expression. **c)** Quantification of S25. **d)** Quantification of *Opa1*, *Snap47*, and *Syt9* qPCR, showing a decrease following OPA1 knockdown. Data shown are mean fold change (N=4) ± SD. Data shown are mean fold change (N=3) ± SD. All data was analysed with a two-tailed, unpaired t-test. ** p<0.01, **** p<0.0001

dose-dependent manner (Li *et al*., 2003). Embryonic neurons were treated with MCL-OM, -Matrix, or a GFP control lentivirus on the day of seeding. At DIV 6, neurons were treated with various doses of rotenone or a DMSO-containing vehicle at various times and cell viability was measured. At all time points and concentrations, excluding 15 nM at 24 hours, MCL1-OM and -Matrix showed significantly higher cell viabilities than the GFP control (**Fig 6a-c**). Furthermore, MCL-Matrix was not significantly different than -OM at any time points or concentrations, suggesting that the Matrix isoform conferred similar protection as the OM isoform, which acts as a traditional anti-apoptotic BCL2 protein. This suggests that manipulating mitochondrial integrity, through MCL1-Matrix, protects post-mitotic neurons against rotenone-induced cell death.

3.4 MCL1-Matrix decreases ATF4 expression after OPA1 knockdown

Now that we have determined that manipulating mitochondrial integrity protects neuronal death, we wanted to ask if manipulating mitochondrial integrity reduces the mitochondrial dysfunction-induced ISR. As previously discussed, many studies have associated the activation of the ISR and ATF4 with the progression of PD (Gully *et al*., 2012; Mercado *et al*., 2018; Demmings *et al*., 2020). Embryonic neurons were treated with MCL1-Matrix, -OM, or GFP as described in section 3.3 with shOPA1 infection on DIV6, and harvested DIV11. Using Atf4 as a readout for ISR activation, we show that MCL1-Matrix significantly reduces Atf4 expression levels by ~37.4% in shOPA1-treated neurons when compared to shOPA1 post-mitotic neurons treated with GFP (**Fig 7a**, **b**). Furthermore, MCL1-OM, which acts mostly in an antiapoptotic manner and previously protected from rotenone-induced apoptosis, reduced in Atf4 expression by ~16.0%, but was not significant ($p = 0.7313$). This suggests that manipulating mitochondrial integrity with MCL1-Matrix reduces mitochondrial dysfunction-induced cell stress.

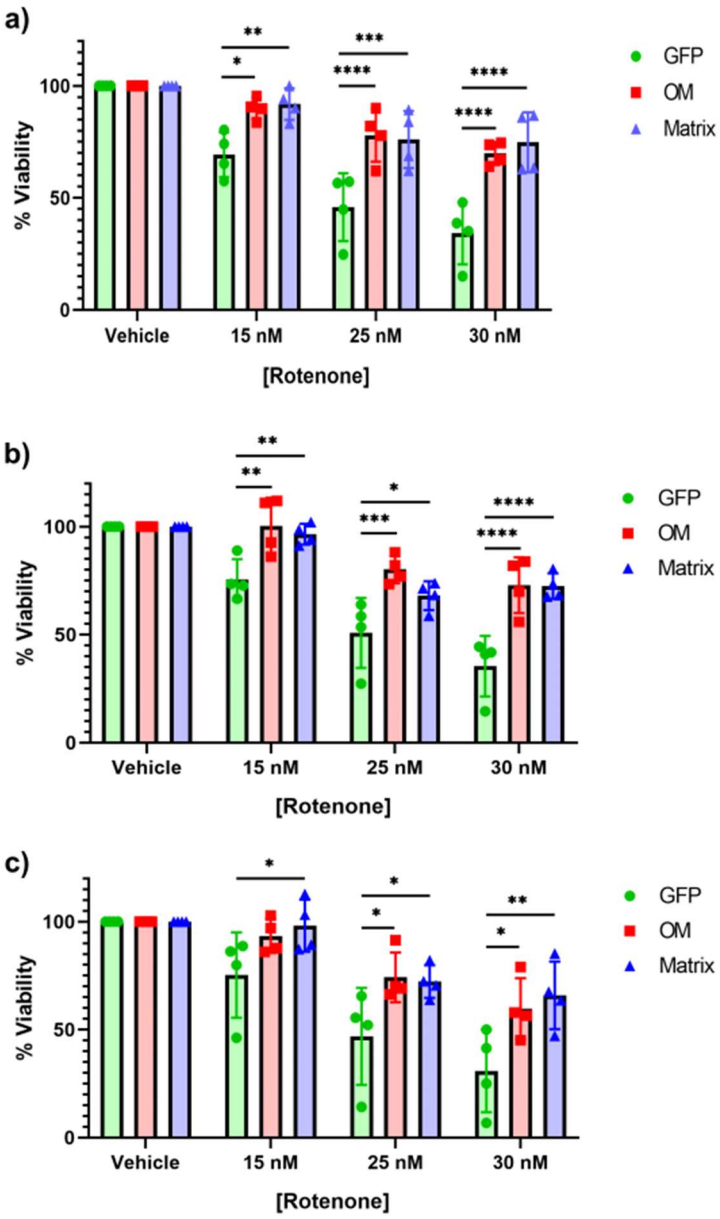

Fig 6. MCL1-OM and -Matrix prevent rotenone-induced cell death. Embryonic neurons (E12-13) were harvested and infected with 5 MOI GFP, MCL1-OM, or MCL1-Matrix on the day of seeding. Neurons were then treated with DMSO containing vehicle, 15 nM, 25 nM, or 30 nM of rotenone on DIV6. Cell viability was determined with an MTS assay after **a)** 6 hours, **b)** 12 hours, and **c)** 24 hours post-rotenone treatment. Data suggests that both MCL1-OM and -Matrix are protective against rotenone-induced cell death. Data shown are mean fold change (N=4) ± SD. Data was analysed with a two-way ANOVA, followed by a Tukey's post-hoc test. * $p<0.05$, ** $p<0.01$, *** $p<0.001$, **** $p<0.0001$

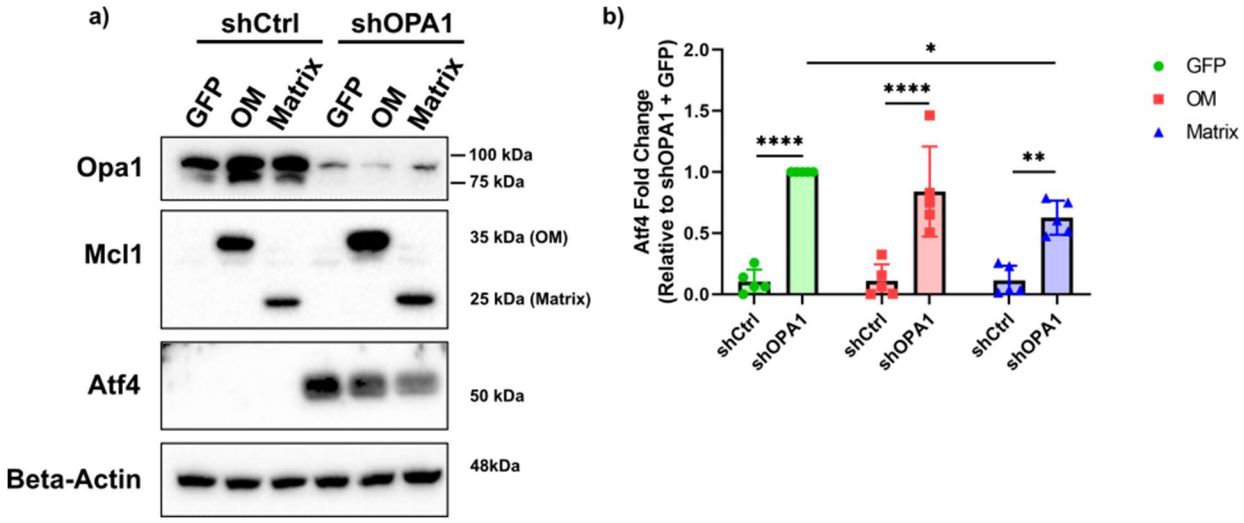

Fig 7. MCL1-Matrix reduces ATF4 expression after OPA1 knockdown a) Embryonic neurons were harvested and infected with 5 MOI GFP, MCL1-OM, or MCL1-Matrix on the day of seeding. Neurons were treated with 5 MOI of shCtrl or shOPA1 on DIV6 and harvested DIV11. Data suggests that MCL1-Matrix significantly decreases OPA1 knockdown-induced ATF4 expression. **b)** Quantification of ATF4. Data shown are mean fold change relative to shOPA1 + GFP (N=5) ± SD. Data was analysed with a two-way ANOVA followed by a Tukey post-hoc test. * $p<0.05$, ** $p<0.01$, **** $p<0.0001$

3.5 MCL1-Matrix decreases ROS production after mitochondrial dysfunction

Having shown that Atf4 is significantly reduced by MCL1-Matrix, we wanted to probe further upstream to determine how MCL1-Matrix reduces stress. As described before, excessive ROS has been associated with the progression of PD and is produced by dysfunctional mitochondria. ROS-induced ER stress leads to the activation of PERK, and subsequent stimulation of the ISR resulting in cell stress and death (Verfaillie *et al*., 2012). MitoSOX red is a fluorophore which primarily reacts and binds to mitochondrial superoxides and is used to quantify the levels of mitochondrial ROS production. To determine if the MCL1 isoforms affect mitochondrial dysfunction-induced ROS, we treated neurons with rotenone at 15 nM for 6 hours, and quantified MitoSOX red intensity. We show rotenone significantly increases mitochondrial ROS production by ~1.548 fold in the GFP treated neurons compared to its DMSO control (**Fig 8a**, **d**, **g**). In OM-treated neurons, rotenone significantly increased the ROS production by ~1.244 fold compared to its control (**Fig 8b**, **e**, **g**). In Matrix-treated neurons, rotenone induced a non-significant increase in ROS production by ~1.156 fold (**Fig 8c**, **f**, **g**). Interestingly, both MCL1 isoforms had significantly less rotenone-induced ROS when compared to GFP neurons treated with rotenone, suggesting that both isoforms confer protection; however, the Matrix isoform does seem to protect at a greater extent.

To further confirm the protective effect of the MCL1 isoforms on mitochondrial dysfunction-induced ROS, we quantified MitoSOX red intensity in OPA1 knockdown neurons. We show a similar pattern to the rotenone-treated samples. Compared to its control, shOPA1 induced a significant upregulation in ROS by ~1.507 fold in GFP treated neurons (**Fig 9a**, **d**, **g**). In OM-treated neurons, OPA1 knockdown significantly increased ROS production by ~1.362 fold compared to its control (**Fig 9b**, **e**, **g**). In Matrix-infect neurons shOPA1, OPA1 knockdown non-

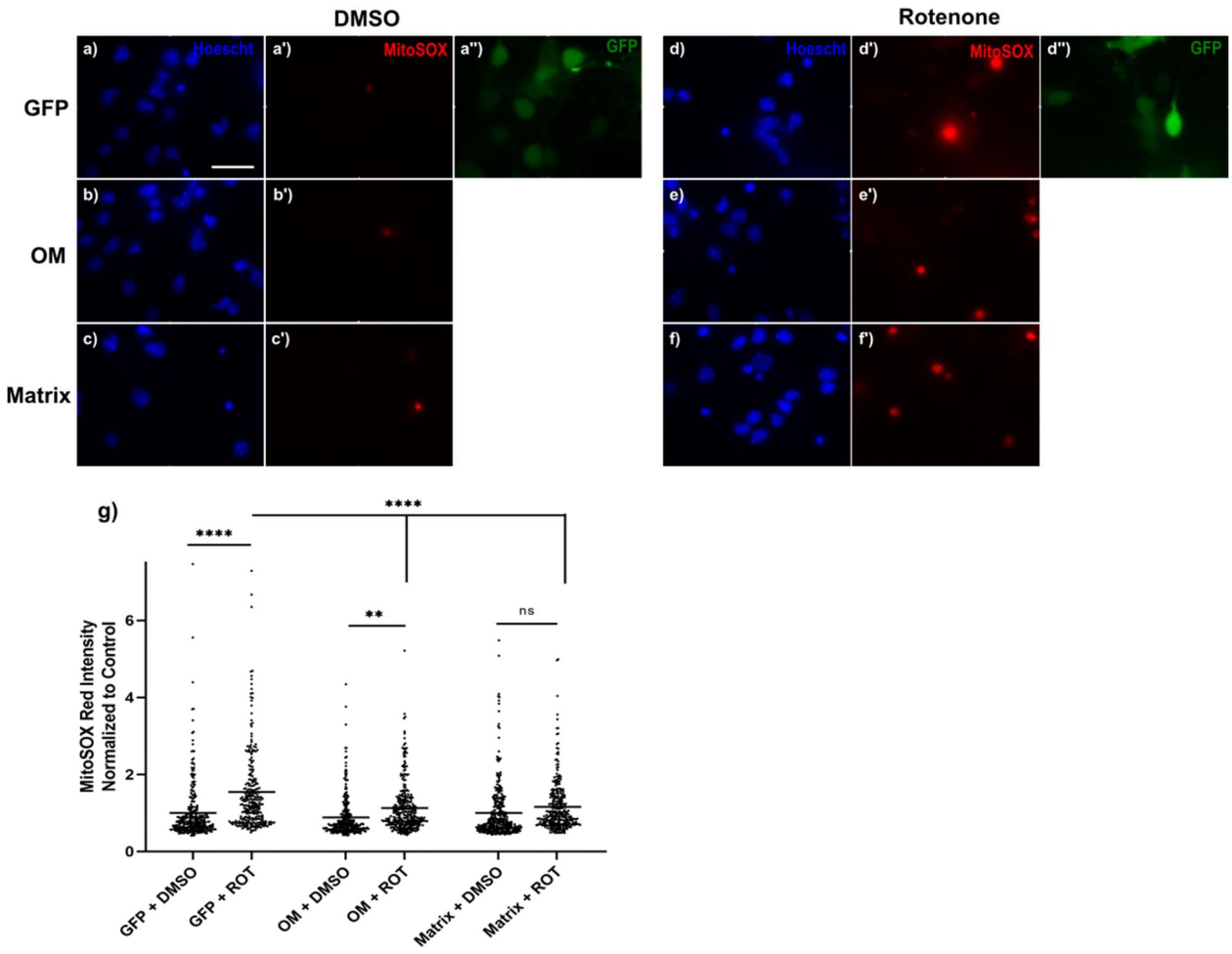

Fig 8. MCL1-Matrix prevents rotenone-induced ROS production. Embryonic neurons were harvested and infected with 5 MOI GFP, MCL1-OM, or MCL1-Matrix on the day of seeding and treated with 15 nM rotenone or DMSO containing vehicle on DIV6. 6 hours post-treatment, cells were incubated with 5 μM of MitoSOX Red. **a-f)** Representative fluorescent images 5 minutes after MitoSOX incubation. Scale bar = 25 μm **g)** Quantification of mean MitoSOX intensity per cell. Data suggests that rotenone does not significantly increase ROS in MCL1-Matrix samples. Both MCL1 isoforms significantly decreased ROS levels compared to GFP + rotenone samples. Data shown is derived from 3 independent experiments with 3 fields each. Data was analysed with a two-way ANOVA, followed by a Tukey's post-hoc test. ** $p<0.01$, **** $p<0.0001$

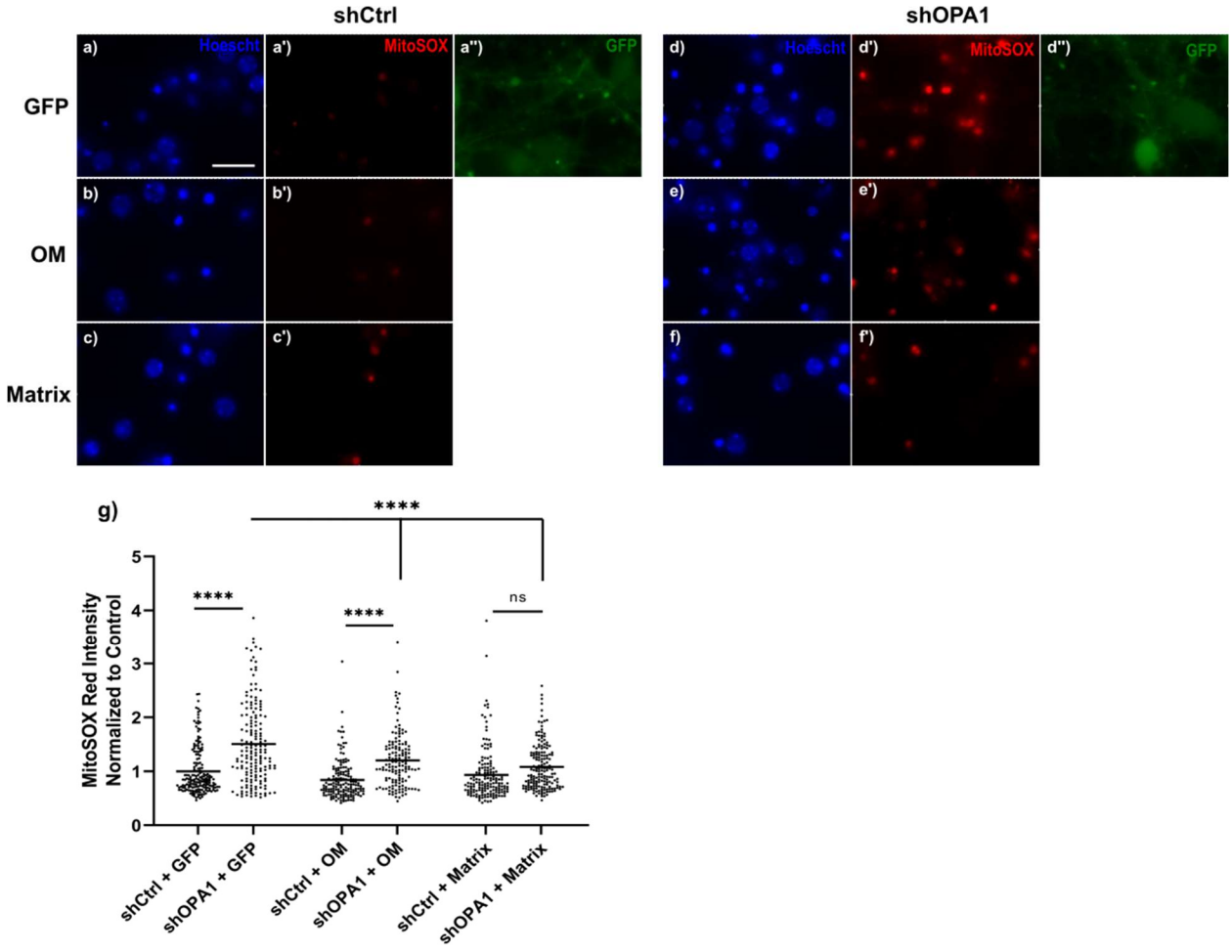

Fig 9. MCL1-Matrix prevents shOPA1-induced ROS production. Embryonic neurons were harvested and infected with 5 MOI GFP, MCL1-OM, or MCL1-Matrix on the day of seeding and infected with 5 MOI shCtrl or shOPA1 on DIV6. On DIV11, cells were incubated with 5 µM of MitoSOX Red. **a-f)** Representative fluorescent images 5 minutes after MitoSOX incubation. Scale bar = 25 µm **g)** Quantification of mean MitoSOX intensity per cell. Data suggests that shOPA1 does not significantly increase ROS in MCL1-Matrix samples. Both MCL1 isoforms significantly decreased ROS levels compared to shOPA1 + GFP samples. Data shown is derived from 3 independent experiments with 3 fields each. Data was analysed with a two-way ANOVA, followed by a Tukey's post-hoc test. **** $p<0.0001$

significantly elevated ROS by ~1.151 fold compared to its control (**Fig 9c**, **f**, **g**). Furthermore, similarly to the rotenone-treated cells, both MCL1 isoforms significantly prevented ROS production compared to the GFP control. This data further reaffirms that the Matrix isoform protects against mitochondrial dysfunction to a greater extent than the OM form. Critically, this demonstrates that reconfiguring mitochondria with MCL1-Matrix protects against mitochondrial dysfunction and stress by preventing excessive ROS production.

DISCUSSION

4.1 Summary of Results

Given the central role of mitochondrial dysfunction in the progression of PD, one would expect that manipulating mitochondrial integrity would reduce neuronal stress and impairments after mitochondrial dysfunction. The goal of this thesis was to determine if enhancing mitochondrial integrity through MCL1-Matrix would effect neuronal stress and protect against cell death in an Opa1 knockdown model of PD. The results of this thesis support a number of conclusions:

1) Knockdown of Opa1 leads to activation of the ISR
2) Knockdown of Opa1 results in the reduction of neuronal gene expression, including those involved in neurotransmission
3) Both MCL1-Matrix and -OM are able to reduce rotenone-induced cell death
4) Manipulating mitochondrial integrity with MCL1-Matrix reduces ATF4 activation
5) MCL1-Matrix reduces mitochondrial ROS after mitochondrial dysfunction

Collectively, these data support the hypothesis that **mitochondrial dysfunction induces stress pathways and is alleviated by manipulating mitochondrial integrity**. Although we show both MCL1 isoforms protect neurons from cell death, due to the MCL1-Matrix's reduction in ROS production and stress gene expression, we can infer that the Matrix isoform exerts its protection by more than just anti-apoptotic activity. Our proposed pathway is summarized in **Figure 10**. The following section discusses the major findings and their implications.

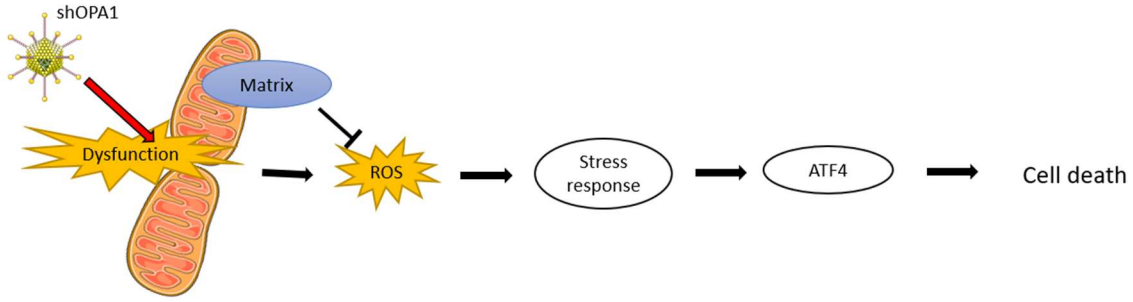

Fig 10. Summary of the proposed pathway. shOPA1-induced mitochondrial dysfunction leads to excessive ROS production and activation of the ISR. This results in mitochondrial dysfunction and cell death. By stabilizing mitochondrial integrity with MCL1-Matrix, ROS levels are reduced, leading to decreased ISR and neuronal protection.

4.1.1 Mitochondrial dysfunction leads to Atf4 expression

Our investigation of the impact of mitochondrial dysfunction in a PD model began with probing for potential stress pathways and impairments on post-mitotic neurons infected with shOPA1 lentivirus (**Fig 4**). Mitochondrial dysfunction, and more specifically, Opa1 knockdown in neurons, lead to deficits including OXPHOS deficiencies, excessive ROS production, and impairment of neuronal function (Iannielli *et al*., 2019; Iannielli *et al*., 2018). By validating results from an RNA bulk sequencing with western blot, we have identified a robust increase in Atf4 expression after Opa1 knockdown, suggesting that the ISR is activated. Additionally, analysis of gene expression by RT-qPCR showed an upregulation of Atf4 downstream targets, *Chop*, *Chac1*, and *Slc7a11*. *Chop* and *Chac1* have been shown to promote apoptosis, while *Slc7a11* has been shown to be upregulated upon oxidative stress. Numerous studies have demonstrated the role of the ISR and ATF4-induced cell death as a player in PD progression (Galehdar *et al*., 2010; Gully *et al*., 2012; Aimé *et al*., 2015; Mercado *et al*., 2018; Yang *et al*., 2019; Aimé *et al*., 2020; Demmings *et al*., 2020). Thus, preventing ISR and ATF4 activation may be a key therapeutic method of slowing PD progression. Importantly, these data suggest that Atf4 can be used as a functional readout for measuring neuronal stress in Opa1 knockdown neurons.

4.1.2 OPA1 knockdown leads to downregulation of synaptic genes

Next, we investigated the impact of mitochondrial dysfunction on neuronal impairment. In PD, DA neurons in post-mortem tissue and animals show deficits in neurotransmitter levels and synaptic communication dysregulation (Galvin and Zivin, 2005; Bereczki *et al*., 2018; Garcia-Reitböck *et al*., 2010; Nemani *et al*., 2010). Interestingly, reduction in the expression of certain synaptic genes involved in exocytosis has been associated with worsening cognition (Berezcki *et*

al., 2018). Particularly in PD and AD, Ca^{2+} sensing, and synaptic vesicle exocytosis have been shown to be impaired (Bereczki *et al*., 2018; Krebs *et al*., 2013). Worsening cognitive decline was associated with lower levels of the Soluble *N*-ethylmaleimide-sensitive factor (NSF) attachment protein receptor (SNARE) complex proteins, Snynaptosomal-associated protein 47 (SNAP47) and synaptic vesicle glycoprotein 2C (SV2C) (Bereczki *et al*., 2018). Another synaptic protein family of interest are the SYTs, a family of proteins regulating synaptic transmission, typically by sensing Ca^{2+} and disassociating from the SNARE complexes, which are shown to be altered under 6-OHDA and levodopa treatments (Galvin and Zivin, 2005; Grushin *et al*., 2019). Based on our preliminary RNA bulk sequencing data, Opa1 knockdown leads to the dysregulation of genes associated with synaptic signaling, vesicle fusion, and exocytosis (**Fig 5a**). To validate these results, we performed immunoblot and RT-qPCR. We showed a downregulation of the SNARE complex genes, Snap25 and *Snap47*, and *Syt9*, a Ca^{2+} sensor, all of which are essential for neurotransmitter release. These data suggest that inducing mitochondrial dysfunction through OPA1 knockdown leads to neuronal impairments which bear certain hallmarks of PD.

4.1.3 MCL1-OM and -Matrix prevent rotenone-induced cell death

Next, we investigated if MCL1 isoforms were able to maintain cell viability when stressed with rotenone, which has been found to induce cell death through apoptosis (Li *et al*., 2003). Our lab has previously reported the protective effects of both MCL1-OM and -Matrix against cell death from NDMA treatment. The Matrix isoform maintained oxygen consumption rate, mitochondrial membrane potential, Ca^{2+} retention, and interacted with complex V to prevent mitochondrial PTP formation (Anilkumar *et al*., 2020). On the other hand, MCL1-OM protected against cell death by sequestering pro-apoptotic BCL2 family proteins (Anilkumar *et al*., 2020; Perciavalle *et al*., 2012). While the OM isoform did show some protective effect on maintaining oxygen consumption rate

and membrane potential, overall, it was not to the extent of the Matrix isoform. We compared the viability of MCL1-Matrix, -OM, and GFP treated neurons after rotenone-induced stress. Rotenone caused a decrease in cell viability, which was prevented with the pre-treatment of either MCL1 isoform (**Fig 6**). Furthermore, there were no significant differences between the Matrix or OM isoforms confirming that they both confer similar protective effects against cell death (Anilkumar *et al*., 2020); however, due to the previously reported differences in their mechanism, this suggests that MCL1-Matrix exerts a protective effect upstream of mitochondrial PTP regulation.

4.1.4 MCL1-Matrix reduces Atf4 expression in shOPA1 neurons

After demonstrating that both MCL1-OM and -Matrix prevent cell death, we decided to investigate the mechanism by which MCL1-Matrix protects dysfunctional neurons. As our lab previously reported that Matrix works upstream of the apoptotic activation, we asked if it had any effect on cell stress. We have shown in **Figure 1**, shOPA1 induces activation of the ISR and upregulation of ATF4. As previously mentioned, ATF4 is suggested to be a key player in PD progression. Thus, we examined if manipulating mitochondrial integrity effected ATF4 expression. We show that MCL1-Matrix significantly reduces Atf4 expression by ~37.0% (**Fig 7**). MCL1-OM non-significantly reduced Atf4 as well, but not to the extent of the Matrix isoform. This suggests that MCL1-Matrix confers a broad protective effect upstream of apoptosis activation by reducing cell stress. Crucially, this again, demonstrates that MCL1-Matrix protects against neuronal dysfunction by a different mechanism than the OM isoform.

4.1.5 MCL1-Matrix decreases ROS production after mitochondrial dysfunction

Lastly, we investigated further upstream to elucidate how MCL1-Matrix is able to protect against cell stress. Mitochondrial dysfunction from OPA1 knockdown and rotenone treatment have

both been shown to induce damaging mitochondrial ROS (Iannielli *et al*., 2018; Khacho *et al*., 2016; Li *et al*., 2003). This ROS production can lead to further mitochondrial damage, activation of the ISR through PERK, and subsequent cell death (Amodio *et al*., 2019; Verfaille *et al*., 2012). Furthermore, excessive ROS as been seen in multiple PD models (Grünewald *et al*., 2019; Inden *et al*., 2011; Kang *et al*., 2009).

To quantify mitochondrial ROS, we used the mitochondrial superoxide indicator, MitoSOX red, and live imaged neurons which were pre-treated with the MCL1 isoforms or a GFP control virus. Inducing mitochondrial dysfunction with rotenone showed an upregulation in mitochondrial ROS by ~1.548 fold (**Fig 8g**). Furthermore, both MCL1-OM and -Matrix isoforms reduced ROS production by ~1.244 and ~1.156 fold, respectively. MCL1-Matrix protected to a greater extent, showing no significant changes between the rotenone and vehicle treated neurons. Mirroring the rotenone-treated neurons, OPA1 knockdown also showed a similar pattern: GFP had increased ROS by ~1.507 fold, whereas MCL-OM and -Matrix only showed a ~1.362 and ~1.151-fold increase, respectively (**Fig 9**). MCL1-Matrix conferred a greater protection compared to -OM, as, again, there were no significant differences between its control and shOPA1 treatment. Taken together, these data suggest that manipulating mitochondrial integrity with MCL1-Matrix reduces cell stress by preventing mitochondrial dysfunction-induced ROS.

Interestingly, while it was to a lesser extent relative to MCL1-Matrix, the OM isoform did reduce ROS and Atf4 expression levels, albeit non-significantly. As an anti-apoptotic BCL2-family protein, MCL1-OM primarily prevents cell death by sequestering BAX (Perciavalle *et al*., 2012); however, Anilkumar *et al*. (2020) demonstrated that in NDMA treated neurons, OM did increase oxygen consumption rate and maintain mitochondrial membrane potential, suggesting that it may exert other protective effects, although not as strong or broad as the Matrix isoform.

This, however, may explain the slight reduction in ROS and Atf4 expression seen in OM-treated cells.

Importantly, we demonstrate that manipulating mitochondrial integrity with MCL1-Matrix protects against mitochondrial dysfunction-induced stress and death by reducing mitochondrial ROS production in neurons. Excessive ROS as been associated with PD progression, particularly in DA neurons of the SN (Grünewald *et al*., 2019; Jin Jung *et al*., 2021; Pacelli *et al*., 2015). By enhancing mitochondrial efficiency with MCL1-Matrix, we can maintain the high bioenergetic requirements of these neurons, while at the same time, preventing further dysfunction by reducing ROS and cell stress-induced death.

4.2 Future Directions

In this thesis, we demonstrated that MCL1-Matrix was able to prevent cell death, reducing ROS production, and cell stress. While this approach characterizes the protective effect against cell stress, we did not characterize Matrix's effects on bioenergetics and supercomplex assembly. OXPHOS impairment and reduced ATP have been shown in many PD models (Bender *et al*., 2006; Pickrell *et al*., 2015; Reeve *et al*., 2013; Iannielli *et al*., 2018). Other studies have demonstrated the MCL1-Matrix ability to maintain oxygen consumption rate, ATP production, and promote supercomplex assembly (Anilkumar *et al*., 2020; Perciavalle *et al*., 2012). Studies have shown the association between OXPHOS impairment and disassembly of ETC supercomplexes in PD models (Lopez-Fauel *et al*., 2017); however, it is still unknown if driving this process will be neuroprotective. Thus, in future experiments, we will determine if MCL1-Matrix induces supercomplex assembly and maintains bioenergetics, and whether these contribute to

neuroprotection, both *in vitro* and *in vivo*. To do this we can turn to blue native blots which allow for the visualization of ETC complexes, and respirometry, which measure oxygen consumption and ATP production. Also, it is evident from previous studies that MCL1-Matrix is able to regulate more than just supercomplex assembly. This prompts the question, how much does supercomplex assembly contribute to the protective effects seen in MCL1-Matrix infected neurons? To isolate the effects of supercomplexes in our model, we can use supercomplex assembly factors such as Cox7RP or (HIG1 Hypoxia Inducible Domain Family Member 2A) HIG2A. These have been shown to increase mitochondrial respiration and promote survival, but no studies have investigated their effects on Ca^{2+}, membrane potential, and stress reduction (Ikeda *et al*., 2019; Balsa *et al*., 2019; Chen *et al*., 2021; Salazar *et al*., 2019).

While MCL1-Matrix and supercomplex assembly are attractive therapeutic targets, we can also look for other potential targets to enhance mitochondrial efficiency. Adenine nucleotide transporter 1 (ANT1) could possibly give rise to a similar protective effect as MCL1-Matrix through a different mechanism. ANT1, also known as ATP/ADP Carrier 1 (AAC1), is an abundant IMM transmembrane protein which exports ATP into the cytosol for usage, and imports ADP into the mitochondria for OXPHOS (Jang *et al*., 2008; Bertholet *et al*., 2019). ANT1 is predominantly expressed in skeletal muscle, the heart, and the brain, whereas other members of the ANT family are expressed in other tissues (Levy *et al*., 2000). Interestingly, ANT1, in particular, does not only regulate ATP transport, but is also involved in regulating the mitochondrial PTP, ETC uncoupling, and mitophagy (Jang *et al*., 2008; Heger *et al*., 2012; Bertholet *et al*., 2019; Hoshino *et al*., 2019). ANT1's role in regulating apoptosis is still unclear. Certain studies have shown that overexpression of ANT1 in cervical, epithelial, and lung cancer cell lines induces mitochondrial PTP opening and subsequent apoptosis (Zamora *et al*., 2004; Jang *et al*., 2008; Zhang *et al*., 2018);

however, overexpressing ANT1 in cardiomyocytes has been shown to decrease cell death and prevent the opening of the mitochondrial PTP through the stabilization of the IMM (Wang *et al*., 2009; Heger *et al*., 2012). Recently, ANT1 has been shown to mediate proton leak across the IMM (Bertholet *et al*., 2019). While, it may seem counterproductive to mitochondrial efficiency, ETC uncoupling can serve to reduce ROS production and subsequent cell damage (Korshunov *et al*., 1997). In fact, it was shown that repression of ANT1 lead to increased ROS production and reduced ATP production (Zhang *et al*., 2017). Knocking out ANT1 reduced uncoupling in cardiomyocytes (Bertholet *et al*., 2019). Furthermore, ANT1-deficient cells had a reduced basal respiration rate. Interestingly, independent of its transporter function, ANT proteins have also been shown to promote mitophagy (Hoshino *et al*., 2019). ANT complexes appear to stabilize PINK1, and loss of ANT proteins resulted in inability to initiate mitophagy in response to oxidative stress. Together, these data suggest that unlike other ATP transporters and uncoupling proteins, ANT1 may act as a master regulator of mitochondrial energy output and quality control, dynamically reacting to the needs of the cell. Like MCL1-Matrix, ANT1 may reduce ROS production while maintaining the energetic requirements of the cell. Manipulating ANT1, in a mitochondrial dysfunction model, may serve as another potential therapeutic target in order to demonstrate the importance of mitochondrial efficiency in PD.

While gene therapy approaches are a powerful tool, restoring mitochondrial efficiency pharmacologically is a rapid method to affirm our data. Recently, the small molecule, mitochondrial fusion promoter hydrazone M1, has been used in a variety of disease models. While it does not directly influence supercomplex assembly, M1 induces mitochondrial fusion by increasing OPA1 and MFN2 expression, resulting in improved cellular respiration (Ding *et al*., 2020; Surinkaew *et al*., 2020). In MFN1 or 2 knockout MEFs, M1 was able to induce

mitochondrial elongation (Wang *et al*., 2012). Furthermore, M1 pre-treatment reduced MPP^+-induced cytochrome c release and cell death in SH-SY5Y cells. In an Alzheimer's disease model, neurons which were pre-treated with M1 induced mitochondrial fusion and reduced ROS accumulation after β-amyloid treatment (Hung *et al*., 2018). In a diabetic cardiomyopathy model, M1 treatment was able to increase OPA1 expression resulting in reduced ROS production, increased oxygen consumption, and reduced cardiomyocyte death (Ding *et al*., 2020). If promoting fusion can protect against PD stressors, it would further underscore the importance of mitochondrial reconfiguration as a potential therapeutic.

This thesis and our previous study have demonstrated the protective effect of MCL1 on *in vitro* models (Anilkumar *et al*., 2020) *In vivo* rescue experiments can be used to determine if MCL1-Matrix is an effective therapeutic in a PD mouse model. We currently have two well studied mouse models, the Parkin/PolG and Thy1-SNCA. The Thy1-SNCA leads to the accumulation of human αSyn in synapses and neurons throughout the brain, within the basal ganglia, substantia nigra, brainstem, and thalamus (Rockenstein *et al*., 2002). These transgenic mice demonstrate several features of PD including early motor deficits and progressive dopamine reduction after 5-6 months, as well as Parkinson-like motor symptoms, DA neuron loss, and reduced survivability after 14 months (Chesselet *et al*., 2012). Parkin/PolG mouse is a PD model which has a proofreading deficiency in PolG, leading to progressive accumulation of mtDNA mutations, and Parkin knockout, preventing effective removal of damaged mitochondria (Pickrell *et al*., 2015). At 52 weeks of age, the mice show loss of DA neurons in the SN and ventral tegmental area and reduced complex I, III, and IV activity (Pickrell et al., 2015). The mice also demonstrated motor impairments which were alleviated by L-DOPA treatment. For adequate delivery of MCL1-Matrix, we have generated AAV8 which has been used for effective and widespread infection in the brain

(Broekman *et al*., 2006; Rousseaux *et al*., 2018). AAV are less immunogenic than other virus types and has been shown to maintain expression for at least a year, making it ideal for manipulating these mouse models (Mays *et al*., 2014; Vassalli *et al*., 2003). To determine the efficacy of MCL1-Matrix, we will investigate at the molecular and behavioral level. At the molecular level, we will examine if Matrix is able to reduce cell stress, protect cell viability, promote supercomplex formation, and maintain energetic requirements. At the behavioral level, efficacy can be assessed through motor tasks, such as the rotorod and pole test. Finally, we can also determine if MCL1 has any effect on survivability. By using MCL1-Matrix in a preclinical PD mouse model, we can determine if reconfiguring mitochondria restores function and promotes survival to provide a novel approach of treating PD.

CONCLUSION

The purpose of this thesis was to briefly characterize stress pathways and neuronal impairment from mitochondrial dysfunction induced by Opa1 knockdown, and then to determine if manipulating mitochondrial integrity with MCL1-Matrix is protective. *In vitro* embryonic neurons treated with shOPA1 resulted in ISR activation, seen by increased expression of ATF4 and its downstream targets, and neuronal impairment, seen by decreased synaptic gene expression. While both MCL1 isoforms, were able to maintain cell viability under rotenone treatment, MCL1-Matrix was found reduce to ISR activation and ROS production to a greater extent. These finding support our hypothesis that stressed induced by mitochondrial dysfunction is alleviated by manipulating mitochondrial integrity. Future studies should focus on investigating if MCL1-Matrix is protective in *in vivo* PD mouse models. Furthermore, future studies can also focus on screening for novel transgenic and pharmacologic targets that manipulate mitochondrial integrity and efficiency. Investigating the efficacy of improving mitochondrial efficiency by preventing neuronal death and enhancing neurological function is a promising direction for the development of novel PD treatments.

REFERENCES

Aimé P, Karuppagounder SS, Rao A, Chen Y, Burke RE, Ratan RR, Greene LA. The drug adaptaquin blocks ATF4/CHOP-dependent pro-death, Trib3 induction and protects in cellular and mouse models of Parkinson's disease. *Neurobiol Dis*. 136: 104725, 2020.

Aimé P, Sun X, Zareen N, Rao A, Berman Z, Volpicelli-Daley L, Bernd P, Crary JF, Levy OA, Greene LA. Trib3 is elevated in Parkinson's disease and mediates death in Parkinson's disease models. *J Neurosci*. 35(30): 10731-10749, 2015.

Aleyasin H, Rousseaux MW, Marcogliese PC, Hewitt SJ, Irrcher I, Joselin AP, Parsanejad M, Kim RH, Rizzu P, Callaghan SM, Slack RS, Mak TW, Park DS. DJ-1 protects the Nigrostriatal axis from the neurotoxin MPTP by modulation of the AKT pathway. *Proc Natl Acad Sci U S A*. 107(7): 3186-3191, 2010.

Amati-Bonneau P, Valentino ML, Reynier P, Gallardo ME, Bornstein B, Boissière A, Campos Y, Rivera H, de la Aleja JG, Carroccia R, Iommarini L, Labauge P, Figarella-Branger D, Marcorelles P, Furby A, Beauvais K, Letournel F, Liguori R, La Morgia C, Montagna P, Liguori M, Zanna C, Rugolo M, Cossarizza A, Wissinger B, Verny C, Schwarzenbacher R, Martín MA, Arenas J, Ayuso C, Garesse R, Lenaers G, Bonneau D, Carelli V. OPA1 mutations induce mitochondrial DNA instability and optic atrophy 'plus' phenotypes. *Brain*. 131(Pt 2): 338-351, 2008.

Amodio G, Moltedo O, Fasano D, Zerillo L, Oliveti M, Di Pietro P, Faraonio R, Barone P, Pellecchia MT, De Rosa A, De Michele G, Polishchuk E, Polishchuk R, Bonifati V, Nitsch L, Pierantoni GM, Renna M, Criscuolo C, Paladino S, Remondelli P. PERK-mediated unfolded protein response activation and oxidative stress in PARK20 fibroblasts. *Front Neurosci*. 13: 673, 2019.

Anilkumar U, Khacho M, Cuillerier A, Harris R, Patten DA, Bilen M, Iqbal MA, Guo DY, Trudeau LE, Park DS, Harper ME, Burelle Y, Slack RS. MCL-1^{Matrix} maintains neuronal survival by enhancing mitochondrial integrity and bioenergetic capacity under stress conditions. *Cell Death Dis*. 11(5): 321, 2020.

Arbour N, Vanderluit JL, Le Grand JN, Jahani-Asl A, Ruzhynsky VA, Cheung ECC, Kelly MA, MacKenzie AE, Park DS, Opferman JT, Slack RS. MCL-1 is a key regulator of apoptosis during CNS development and after DNA damage. *J Neurosci*. 28(24): 6068-6078, 2008.

Armstrong MJ, Okun MS. Diagnosis and treatment of Parkinson disease: a review. *JAMA*. 323(6): 548-560, 2020.

Bai X, Ni J, Beretov J, Wasinger VC, Wang S, Zhu Y, Graham P, Li Y. Activation of the eIF2α/ATF4 axis drives triple-negative breast cancer radioresistance by promoting glutathione biosynthesis. *Redox Biol*. 43: 101993, 2021.

Balsa E, Soustek MS, Thomas A, Cogliati S, García-Poyatos C, Martín-García E, Jedrychowski M, Gygi SP, Enriquez JA, Puigserver P. ER and nutrient stress promote assembly of respiratory chain supercomplexes through the PERK-eIF2α axis. *Mol Cell*. 74(5): 877-890, 2019.

Bender A, Krishnan KJ, Morris CM, Taylor GA, Reeve AK, Perry RH, Jaros E, Hersheson JS, Betts J, Klopstock T, Taylor RW, Turnbull DM. High levels of mitochondrial DNA deletions in Substantia Nigra neurons in aging and Parkinson disease. *Nat Genet*. 38(5): 515-517, 2006.

Bereczki E, Branca RM, Francis PT, Pereira JB, Baek JH, Hortobágyi T, Winblad B, Ballard C, Lehtiö J, Aarsland D. Synaptic markers of cognitive decline in neurodegenerative diseases: a proteomic approach. *Brain*. 141(2): 582-595, 2018.

Bereczki E, Francis PT, Howlett D, Pereira JB, Höglund K, Bogstedt A, Cedazo-Minguez A, Baek JH, Hortobágyi T, Attems J, Ballard C, Aarsland D. Synaptic proteins predict cognitive decline in Alzheimer's disease and Lewy body dementia. *Alzheimers Dement*. 12(11): 1149-1158, 2016.

Bertholet AM, Chouchani ET, Kazak L, Angelin A, Fedorenko A, Long JZ, Vidoni S, Garrity R, Cho J, Terada N, Wallace DC, Spiegelman BM, Kirichok Y. H+ transport is an integral function of the mitochondrial ADP/ATP carrier. *Nature*. 571(7766): 515-520, 2019.

Bertrand E, Lechowicz W, Szpak GM, Dymecki J. Qualitative and quantitative analysis of locus coeruleus neurons in Parkinson's disease. *Folia Neuropathol*. 35(2): 80-96, 1997.

Bonifati V, Rizzu P, van Baren MJ, Schaap O, Breedveld GJ, Krieger E, Dekker MC, Squitieri F, Ibanez P, Joosse M, van Dongen JW, Vanacore N, van Swieten JC, Brice A, Meco G, van Duijn CM, Oostra BA, Heutink P. Mutations in the DJ-1 gene associated with autosomal recessive early-onset parkinsonism. *Science*. 299(5604): 256-259, 2003.

Broekman ML, Comer LA, Hyman BT, Sena-Esteves M. Adeno-associated virus vectors serotyped with AAV8 capsid are more efficient than AAV-1 or -2 serotypes for widespread gene delivery to the neonatal mouse brain. *Neuroscience*. 138(2): 501-510, 2006.

Buchman AS, Shulman JM, Nag S, Leurgans SE, Arnold SE, Morris MC, Schneider JA, Bennett DA. Nigral pathology and parkinsonian signs in elders without Parkinson disease. *Ann Neurol*. 71(2): 258-266.

Burbulla LF, Song P, Mazzulli JR, Zampese E, Wong YC, Jeon S, Santos DP, Blanz J, Obermaier CD, Strojny C, Savas JN, Kiskinis E, Zhuang X, Krüger R, Surmeier DJ, Krainc D. Dopamine oxidation mediates mitochondrial and lysosomal dysfunction in Parkinson's disease. *Science*. 357(6357): 1255-1261, 2017.

Callizot N, Combes M, Henriques A, Poindron P. Necrosis, apoptosis, necroptosis, three modes of action of dopaminergic neuron neurotoxins. *PLoS One*. 14(4): e0215277, 2019.

Carelli V, Musumeci O, Caporali L, Zanna C, La Morgia C, Del Dotto V, Porcelli AM, Rugolo M, Valentino ML, Iommarini L, Maresca A, Barboni P, Carbonelli M, Trombetta C, Valente EM, Patergnani S, Giorgi C, Pinton P, Rizzo G, Tonon C, Lodi R, Avoni P Liguori R Baruzzi A, Toscano A, Zeviani M. Syndromic parkinsonism and dementia associated with OPA1 missense mutations. *Ann Neurol*. 78(1): 21-38, 2015.

Cartron PF, Gallenne T, Bougras G, Gautier F, Manero F, Vusio P, Meflah K, Vallette FM, Juin P. The first alpha helix of Bax plays a necessary role in its ligand-induced activation by the BH3-only proteins Bid and PUMA. *Mol Cell*. 16(5): 807-818, 2004.

Certo M, Del Gaizo Moore V, Nishino M, Wei G, Korsmeyer S, Armstrong SA, Letai A. Mitochondria primed by death signals determine cellular addiction to antiapoptotic BCL-2 family members. *Cancer Cell*. 9(5): 351-65, 2006.

Chen S, Dai Y, Harada H, Dent P, Grant S. Mcl-1 down-regulation potentiates ABT-737 lethality by cooperatively inducing Bak activation and Bax translocation. *Cancer Res*. 67: 782–791, 2005.

Chen H, Detmer SA, Ewald AJ, Griffin EE, Fraser SE, Chan DC. Mitofusins Mfn1 and Mfn2 coordinately regulate mitochondrial fusion and are essential for embryonic development. *J Cell Biol*. 160(2): 189-200, 2003.

Chen H, Xu J, Lv Y, He P, Liu C, Jiao J, Li S, Mao X, Xue X. Proanthocyanidins exert a neuroprotective effect via ROS/JNK signaling in MPTP-induced Parkinson's disease models in vitro and in vivo. *Mol Med Rep*. 18(6): 4913-4921, 2018.

Cheng HC, Ulane CM, Burke RE. Clinical progression in Parkinson disease and the neurobiology of axons. *Ann Neurol*. (6): 715-725, 2010.

Chesselet M-F, Richter F, Zhu C, Magen I, Watson MB, Subramaniam SR. A progressive mouse model of Parkinson's disease: the Thy1-aSyn ("Line 61") mice. *Neurotherapeutics*. 9(2): 297-314, 2012.

Chia SJ, Tan E-K, Chao Y-X. Historical perspective: models of Parkinson’s disease. *Int J Mol Sci*. 21(7): 2464, 2020.

Circu ML, Moyer MP, Harrison L, Aw TY. Contribution of glutathione status to oxidant-induced mitochondrial DNA damage in colonic epithelial cells. *Free Radic Biol Med*. 47(8): 1190-1198, 2009.

Cogliati S, Calvo E, Loureiro M, Guaras AM, Nieto-Arellano R, Garcia-Poyatos C, Ezkurdia I, Mercader N, Vázquez J, Enriquez JA. Mechanism of super-assembly of respiratory complexes III and IV. *Nature*. 539(7630): 579-582, 2016.

Cogliati S, Frezza C, Soriano ME, Varanita T, Quintana-Cabrera R, Corrado M, Cipolat S, Costa V, Casarin A, Gomes LC, Perales-Clemente E, Salviati L, Fernandez-Silva P, Enriquez JA, Scorrano L. Mitochondrial cristae shape determines respiratory chain supercomplexes assembly and respiratory efficiency. *Cell*. 155(1): 160-171, 2013.

Chen YC, Taylor EB, Dephoure N, Heo JM, Tonhato A, Papandreou I, Nath N, Denko NC, Gygi SP, Rutter J. Identification of a protein mediating respiratory supercomplex stability. *Cell Metab*. 15(3): 348-360, 2012.

Chung C, Raingo J. Vesicle dynamics: how synaptic proteins regulate different modes of neurotransmission. *J Neurochem*. 126(2): 146-154, 2013.

Dai Y, Kiselak T, Clark J, Clore E, Zheng K, Cheng A, Kijoth GC, Prolla TA, Maratos-Flier E, Simon DK. Behavioral and metabolic characterization of heterozygous and homozygous POLG mutator mice. *Mitochondrion*. 13(4): 282-291, 2013.

Demmings MD, Tennyson EC, Petroff GN, Tarnowski-Garner HE, Cregan SP. Activating transcription factor-4 promotes neuronal death induced by Parkinson's disease neurotoxins and α-synuclein aggregates. *Cell Death Differ*. 28(5): 1627-1643, 2021.

Ding M, Liu C, Shi R, Yu M, Zeng K, Kang J, Fu F, Mi M. Mitochondrial fusion promoter restores mitochondrial dynamics balance and ameliorates diabetic cardiomyopathy in an optic atrophy 1-dependent way. *Acta Physiol (Oxf)*. 229(1): e13428, 2020.

Do Van B, Gouel F, Jonneaux A, Timmerman K, Gelé P, Pétrault M, Bastide M, Laloux C, Moreau C, Bordet R, Devos D, Devedjian JC. Ferroptosis, a newly characterized form of cell death in Parkinson's disease that is regulated by PKC. *Neurobiol Dis*. 94: 169-178, 2016.

Du H, Guo L, Yan S, Sosunov AA, McKhann GM, Yan SS. Early deficits in synaptic mitochondria in an Alzheimer's disease mouse model. *Proc Natl Acad Sci U S A*. 107(43): 18670-18675, 2010.

Dzhagalov I, Dunkle A, He YW. The anti-apoptotic Bcl-2 family member Mcl-1 promotes T lymphocyte survival at multiple stages. *J Immunol*. 181(1): 521-528, 2008.

Elmore S. Apoptosis: a review of programmed cell death. *Toxicol Pathol*. 35(4): 495-516, 2007.

Fogarty LC, Flemmer RT, Geizer BA, Licursi M, Karunanithy A, Opferman JT, Hirasawa K, Vanderluit JL. Mcl-1 and Bcl-xL are essential for survival of the developing nervous system. *Cell Death Differ*. 26(8): 1501-1515, 2019.

Frezza C, Cipolat S, Martins de Brito O, Micaroni M, Beznoussenko GV, Rudka T, Bartoli D, Polishuck RS, Danial NN, De Strooper B, Scorrano L. OPA1 controls apoptotic cristae remodeling independently from mitochondrial fusion. *Cell*. 126(1): 177-189, 2006.

Galehdar Z, Swan P, Fuerth B, Callaghan SM, Park DS, Cregan SP. Neuronal apoptosis mediated by endoplasmic reticulum stress is regulated by ATF4-CHOP-mediated induction of Bcl-2 homology 3-only member PUMA. *J Neurosci*. 30(15): 16938-16948, 2010.

Garcia-Reitböck P, Anichtchik O, Bellucci A, Iovino M, Ballini C, Fineberg E, Ghetti B, Della Corte L, Spano P, Tofaris GK, Goedert M, Spillantini MG. SNARE protein redistribution and synaptic failure in a transgenic mouse model of Parkinson's disease. *Brain*. 133(Pt 7): 2032-2044, 2010.

Gerfen CR, Surmeier DJ. Modulation of striatal projection systems by dopamine. *Annu Rev Neurosci*. 34: 441-466, 2011.

Germain M, Nguyen AP, Le Grand JN, Arbour N, Vanderluit JL, Park DS, Opferman JT, Slack RS. MCL-1 is a stress sensor that regulates autophagy in a developmentally regulated manner. *EMBO J*. 30(2): 395-407, 2011.

Glavin G, Zivin M. Differential expression of striatal synaptotagmin mRNA isoforms in hemiparkinsonian rats. *Neuroscience*. 135(2): 545-554, 2005.

Glytsou C, Calvo E, Cogliati S, Mehrota A, Anastasia I, Rigoni G, Raimondi A, Shintani N, Loureiro M, Vasquez J, Pellegrini L, Enriquez JA, Scorrano L, Soriano ME. Optic atrophy 1 is epistatic to the core MICOS component MIC60 in mitochondrial cristae shape control. *Cell Rep*. 17(11): 3024-3034, 2016.

Gomes LC, Di Benedetto G, Scorrano L. During autophagy mitochondria elongate, are spared from degradation and sustain cell viability. *Nat Cell Biol*. 13(5): 589-598, 2011.

Grünewald A, Kumar KR, Sue CM. New insights into the complex role of mitochondria in Parkinson's disease. *Prog Neurobiol*. 177: 73-93, 2019.

Grushin K, Wang J, Coleman J, Rothman JE, Sindelar CV, Krishnakumar SS. Structural basis for the clamping and Ca2+ activation of SNARE-mediated fusion by synaptotagmin. *Nat Commun*. 10(1): 2413, 2019.

Guo R, Zong S, Wu M, Gu J, Yang M. Architecture of human mitochondrial respiratory megacomplex $I_2III_2IV_2$. *Cell*. 170(6): 1247-1257.e12, 2017.

Han H, Tan J, Wang R, Wan H, He Y, Yan X, Guo J, Gao Q, Li J, Shang S, Chen F, Tian R, Liu W, Liao L, Tang B, Zhang Z. PINK1 phosphorylates Drp1S616 to regulate mitophagy-independent mitochondrial dynamics. *EMBO Rep*. 21(8): e48686, 2020.

Hattori N, Kitada T, Matsumine H, Asakawa S, Yamamura Y, Yoshino H, Kobayashi T, Yokochi M, Wang M, Yoritaka A, Kondo T, Kuzuhara S, Nakamura S, Shimizu N, Mizuno Y. Molecular genetic analysis of a novel Parkin gene in Japanese families with autosomal recessive juvenile parkinsonism: evidence for variable homozygous deletions in the Parkin gene in affected individuals. *Ann Neurol*. 44(6): 935-941, 1998.

Heger J, Abdallah Y, Shahzad T, Klumpe I, Piper HM, Schultheiss HP, Schlüter KD, Schulz R, Euler G, Dörner A. Transgenic overexpression of the adenine nucleotide translocase 1 protects cardiomyocytes against TGFβ1-induced apoptosis by stabilization of the mitochondrial permeability transition pore. *J Mol Cell Cardiol*. 53(1): 73-81, 2012.

Henderson JM, Carpenter K, Cartwright H, Halliday GM. Degeneration of the centre median-parafascicular complex in Parkinson's disease. *Ann Neurol*. 47: 345–452, 2000.

Hoshino A, Wang W-J, Wada S, McDermott-Roe C, Evans CS, Gosis B, Morley MP, Rathi KS, Li J, Li K, Yang S, McManus MJ, Bowman C, Potluri P, Levin M, Damrauer S, Wallace DC, Holzbaur ELF, Arany Z. The ADP/ATP translocase drives mitophagy independent of nucleotide exchange. *Nature*. 575(7782): 375-379, 2019.

Huang CR, Yang-Yen HF. The fast-mobility isoform of mouse Mcl-1 is a mitochondrial matrix-localized protein with attenuated anti-apoptotic activity. *FEBS Lett*. 584(15): 3323-3330, 2010.

Hung CH, Cheng SS, Cheung YT, Wuwongse S, Zhang NQ, Ho Y-S, Lee SM, Chang RC. A reciprocal relationship between reactive oxygen species and mitochondrial dynamics in neurodegeneration. *Redox Biol*. 14:7-19, 2018.

Iannielli A, Bido S, Folladori L, Segnali A, Cancellieri C, Maresca A, Massimino L, Rubio A, Morabito G, Caporali L, Tagliavini F, Musumeci O, Gregato G, Bezard E, Carelli V, Tiranti V, Broccoli V. Pharmacological inhibition of necroptosis protects from dopaminergic neuronal cell death in Parkinson's disease models. *Cell Rep*. 22(8): 2006-2079, 2018.

Iannielli A, Ugolini GS, Cordiglieri C, Bido S, Rubio A, Colasante G, Valtorta M, Cabassi T, Rasponi M, Broccoli V. Reconstitution of the human Nigro-striatal pathway on-a-chip reveals OPA1-dependent mitochondrial defects and loss of dopaminergic synapses. *Cell Rep*. 29(13): 4646-4656, 2019.

Inden M, Kitamura Y, Abe M, Tamaki A, Takata K, Taniguchi T. Parkinsonian rotenone mouse model: reevaluation of long-term administration of rotenone in C57BL/6 mice. *Biol Pharm Bull*. 34(1): 92-96, 2011.

Inoue Y, Hara H, Mitsugi Y, Yamaguchi E, Kamiya T, Itoh A, Adachi T. 4-Hydroperoxy-2-decenoic acid ethyl ester protects against 6-hydroxydopamine-induced cell death via activation of Nrf2-ARE and eIF2α-ATF4 pathways. *Neurochem Int*. 112: 288-296, 2018.

Jang JY, Choi Y, Jeon YK, Aung KC, Kim CW. Over-expression of adenine nucleotide translocase 1 (ANT1) induces apoptosis and tumor regression in vivo. *BMC Cancer*. 8: 160, 2008

Javitch JA, D'Amato RJ, Strittmatter SM, Snyder SH. Parkinsonism-inducing neurotoxin, *N*-methyl-4-phenyl-1,2,3,6-tetrahydropyridine: uptake of the metabolite *N*-methyl-4-phenylpyridine by dopamine neurons explains selective toxicity. *Proc Natl Acad Sci U S A*. 82(7): 2173-2177, 1985.

Jin Jung Y, Choi H, Oh E. Effects of particulate matter and nicotine for the MPP+-induced SH-SY5Y cells: Implication for Parkinson's disease. *Neurosci Lett*. 765: 136265, 2021.

Judge A, Dodd MS. Metabolism. *Essays Biochem*. 64(4): 607-647, 2020.

Kang MJ, Gil SJ, Koh HC. Paraquat induces alternation of the dopamine catabolic pathways and glutathione levels in the substantia nigra of mice. *Toxicol Lett*. 188(2): 148-152, 2009.

Khacho M, Clark A, Svoboda DS, Azzi J, MacLaurin JG, Meghaizel C, Sesaki H, Lagace DC, Germain M, Harper M-E, Park DS, Slack RS. Mitochondrial dynamics impacts stem cell identity and fate decisions by regulating a nuclear transcription program. *Cell Stem Cell*. 19(2): 232-247, 2016.

Khacho M, Tarabay M, Patten D, Khacho P, MacLaurin JG, Guadagno J, Bergeron R, Cregan SP, Harper M-E, Park DS, Slack RS. Acidosis overrides oxygen deprivation to maintain mitochondrial function and cell survival. *Nat Commun.* 5: 3550, 3014.

Kim RH, Smith PD, Aleyasin H, Hayley S, Mount MP, Pownall S, Wakeham A, You-Ten AJ, Kalia SK, Horne P, Westaway D, Lozano AM, Anisman H, Park DS, Mak TW. Hypersensitivity of DJ-1-deficient mice to 1-methyl-4-phenyl-1,2,3,6-tetrahydropyrindine (MPTP) and oxidative stress. *Proc Natl Acad Sci U S A*. 102(14): 5215-5220, 2005.

Kojima E, Takeuchi A, Haneda M, Yagi A, Hasegawa T, Yamaki K, Takeda K, Akira S, Shimokata K, Isobe K. The function of GADD34 is a recovery from shutoff of protein synthesis induced by ER stress: elucidation by GADD34 deficient mice. *FASEB J*. 17(11): 1573-1575, 2003.

Korobova F, Ramabhadran V, Higgs HN. An actin-dependent step in mitochondrial fission mediated by the ER-associated formin INF2. *Science*. 339(6118): 464-467, 2013.

Korshunov SS, Skulachev VP, Starkov AA. High protonic potential actuates a mechanism of production of reactive oxygen species in mitochondria. *FEBS Lett*. 416(1): 15-18, 1997.

Kuwana T, Bouchier-Hayes L, Chipuk JE, Bonzon C, Sullivan BA, Green DR, Newmeyer DD. BH3 domains of BH3-only proteins differentially regulate Bax-mediated mitochondrial membrane permeabilization both directly and indirectly. *Mol Cell*. 17(4): 525-535, 2005.

Lanciego JL, Luquin N, Obeso JA. Functional neuroanatomy of the basal ganglia. *Cold Spring Harb Perspect Med*. 2(12): a009621, 2012.

Lee H, Smith SB, Yoon Y. The short variant of the mitochondrial dynamin OPA1 maintains mitochondrial energetics and cristae structure. *J Biol Chem*. 292(17): 7115-7130, 2017.

Lemaire PA, Anderson E, Lary J, Cole JL. Mechanism of PKR activation of dsRNA. *J Mol Biol*. 381(2): 351-360, 2008.

Letai A, Bassik MC, Walensky LD, Sorcinelli MD, Weiler S, Korsmeyer SJ. Distinct BH3 domains either sensitize or activate mitochondrial apoptosis, serving as prototype cancer therapeutics. *Cancer Cell*. 2(3): 183-192, 2002.

Levites Y, Jansen K, Smithson LA, Dakin R, Holloway VM, Das P, Golde TE. Intracranial adeno-associated virus-mediated delivery of anti-pan amyloid beta, amyloid beta40, and amyloid beta42 single-chain variable fragments attenuates plaque pathology in amyloid precursor protein mice. *J Neurosci*. 26(46): 11923-11928, 2006.

Levy SE, Chen YS, Graham BH, Wallace DC. Expression and sequence analysis of the mouse adenine nucleotide translocase 1 and 2 genes. *Gene*. 254(1-2): 57-66, 2000.

Li N, Ragheb K, Lawler G, Sturgis J, Rajwa B, Melendez JA, Robinson JP. Mitochondrial complex I inhibitor rotenone induces apoptosis through enhancing mitochondrial reactive oxygen species production. *J Biol Chem*. 278(10): 8516-8525, 2003.

Liao C, Ashley N, Diot A, Morten K, Phadwal K, Williams A, Fearnley I, Rosser L, Lowndes J, Fratter C, Ferguson DJ, Vay L, Quaghebeur G, Moroni I, Bianchi S, Lamperti C, Downes SM, Sitarz KS, Flannery PJ, Carver J, Dombi E, East D, Laura M, Reilly MM, Mortiboys H, Prevo R, Campanella M, Daniels MJ, Zeviani M, Yu-Wai-Man P, Simon AK, Votruba M, Poulton J.

Dysregulated mitophagy and mitochondrial organization in optic atrophy due to OPA1 mutations. *Neurology*. 88(2): 131-142, 2017.

Livak KJ, Schmittgen TD. Analysis of relative gene expression data using real-time quantitative PCR and the $2^{-\Delta\Delta C}_{T}$ method. *Methods*. 25(4): 402-408, 2001.

Lobo-Jarne T, Pérez-Pérez R, Fontanesi F, Timón-Gómez A, Wittig I, Peñas A, Serrano-Lorenzo P, García-Consuegra I, Arenas J, Martín MA, Barrientos A, Ugalde C. Multiple pathways coordinate assembly of human mitochondrial complex IV and stabilization of respiratory supercomplexes. *EMBO J*. 39(14): e103912, 2020.

Longchamp A, Mirabella T, Arduini A, MacArthur MR, Das A, Treviño-Villarreal JH, Hine C, Ben-Sahra I, Knudsen NH, Brace LE, Reynolds J, Mejia P, Tao M, Sharma G, Wang R, Corpataux J-M, Haefliger J-A, Ahn KH, Lee C-H, Manning BD, Sinclair DA, Chen CS, Ozaki CK, Mitchell JR. Amino acid restriction triggers angiogenesis via GCN2/ATF4 regulation of VEGF and H_2S. *Cell*. 173(1): 117-129, 2018.

Lopez H, Zhang L, George NM, Liu X, Pang X, Evans JJD, Targy NM, Luo X. Perturbation of the Bcl-2 network and an induced Noxa/Bcl-xL interaction trigger mitochondrial dysfunction after DNA damage. *J Biol Chem*. 285(20): 15016-15026, 2010.

Lopez-Fabuel I, Martin-Martin L, Resch-Beusher M, Azkona G, Sanchez-Pernaute R, Bolaños JP. Mitochondrial respiratory chain disorganization in Parkinson's disease-relevant PINK1 and DJ1 mutants. *Neurochem Int*. 109: 101-105, 2017.

Losón OC, Song Z, Chen H, Chan DC. Fis1, Mff, MiD49, and MiD51 mediate Drp1 recruitment in mitochondrial fission. *Mol Biol Cell*. 24(5): 659-667, 2013.

Mailloux RJ, McBride SL, Harper M-L. Unearthing the secrets of mitochondrial ROS and glutathione in bioenergetics. *Trends Biochem Sci*. 38(12): 592-602, 2013.

Martí Y, Matthaeus F, Lau T, Schloss P. Methyl-4-phenylpyridinium (MPP^+) differentially affects monoamine release and re-uptake in murine embryonic stem cell-derived dopaminergic and serotonergic neurons. *Mol Cell Neurosci*. 83: 37-45, 2017.

Matheoud D, Sugiura A, Bellemare-Pelletier A, Laplante A, Rondeau C, Chemali M, Fazel A, Bergeron JJ, Trudeau L-E, Burelle Y, Gagnon E, McBride HM, Desjardins M. Parkinson's disease-related proteins PINK1 and Parkin repress mitochondrial antigen presentation. *Cell*. 166(2): 314-327, 2016.

Matsuda N, Sato S, Shiba K, Okatsu K, Saisho K, Gautier CA, Sou YS, Saiki S, Kawajiri S, Sato F, Kimura M, Komatsu M, Hattori N, Tanaka K. PINK1 stabilized by mitochondrial depolarization recruits Parkin to damaged mitochondria and activates latent Parkin for mitophagy. *J Cell Biol*. 189(2): 211-221, 2010.

Mays LE, Wang L, Lin J, Bell P, Crawford A, Wherry EJ, Wilson JM. AAV8 induces tolerance in murine muscle as a result of poor APC transduction, T cell exhaustion, and minimal MHCI upregulation on target cells. *Mol Ther*. 22(1): 28-41, 2014.

McRitchie DA, Cartwright HR, Halliday GM. Specific A10 dopaminergic nuclei in the midbrain degenerate in Parkinson's disease. *Exp Neurol*. 144:202–213, 1997.

Mercado G, Castillo V, Soto P, López N, Axten JM, Sardi SP, Hoozemans JJM, Hetz C. Targeting PERK signaling with the small molecule GSK2606414 prevents neurodegeneration in a model of Parkinson's disease. Neurobiol Dis. 112: 136-148, 2018.

Mitra K, Wunder C, Roysam B, Lin G, Lippincott-Schwartz J. A hyperfused mitochondrial state achieved at G1-S regulates cyclin E buildup and entry into S phase. *Proc Natl Acad Sci U S A*. 106(29): 11960-11965, 2009.

Murphy MP. Mitochondrial thiols in antioxidant protection and redox signaling: distinct roles for glutathionylation and other thiol modifications. *Antioxid Redox Signal*. 16(6): 476-495, 2012.

Narendra DP, Jin SM, Tanaka A, Suen DF, Gautier CA, Shen J, Cookson MR, Youle RJ. PINK1 is selectively stabilized on impaired mitochondria to activate Parkin. *PLoS Biol*. 8(1): e1000298, 2010.

Nakahira K, Haspel JA, Rathinam VA, Lee SJ, Dolinay T, Lam HC, Englert JA, Rabinovitch M, Cernadas M, Kim HP, Fitzgerald KA, Ryter SW, Choi AM. Autophagy proteins regulate innate immune responses by inhibiting the release of mitochondrial DNA mediated by the NALP3 inflammasome. *Nat Immunol*. 12(3): 222-230, 2011.

Nemani VM, Lu W, Berge V, Nakamura K, Onoa B, Lee MK, Chaudhry FA, Nicoll RA, Edwards RH. Increased expression of alpha-synuclein reduces neurotransmitter release by inhibiting synaptic vesicle reclustering after endocytosis. *Neuron*. 65(1): 66-79, 2010.

Niso-Santano M, González-Polo RA, Bravo-San Pedro JM, Gómez-Sánchez R, Lastres-Becker I, Ortiz-Ortiz MA, Soler G, Morán JM, Cuadrado A, Fuentes JM; Centro de Investigación Biomédica en Red sobre Enfermedades Neurodegenerativas (CIBERNED). Activation of apoptosis signal-regulating kinase 1 is a key factor in paraquat-induced cell death: modulation by the Nrf2/Trx axis. *Free Radic Biol Med*. 48(10): 1370-1381, 2010.

Nolfi-Donegan D, Braganza A, Shiva S. Mitochondrial electron transport chain: Oxidative phosphorylation, oxidation production, and methods of measurement. *Redox Biol*. 37: 101674, 2020.

Nunnari J, Suomalainen A. Mitochondria: In sickness and in health. *Cell*. 148(6): 1145-1159, 2012.

Obeso JA, Rodríguez-Oroz MC, Benitez-Temino B, Blesa FJ, Guridi J, Marin C, Rodriguez M. Functional organization of the basal ganglia: therapeutic implications for Parkinson's disease. *Mov Disord*. Suppl 3: S548-559, 2008.

Okun MS. Deep-brain stimulation for Parkinson’s disease. *N Engl J Med*. 367(16): 1529-1538, 2012.

Pacelli C, Giguère N, Bourque MJ, Lévesque M, Slack RS, Trudeau LÉ. Elevated mitochondrial bioenergetics and axonal arborization size are key contributors to the vulnerability of dopamine neurons. *Curr Biol*. 25(18): 2349-2360, 2015.

Pacifici F, Salimei C, Pastore D, Malatesta G, Ricordi C, Donadel G, Bellia A, Rovella V, Tafani M, Garaci E, Tesauro M, Lauro D, Di Daniele N, Della-Morte D. The protective effect of a unique mix of polyphenols and micronutrients against neurodegeneration induced by an in vitro model of Parkinson's disease. *Int J Mol Sci*. 23(6): 3110, 2022.

Pakos-Zebrucka K, Koryga I, Mnich K, Ljujic M, Samali A, Gorman AM. The integrated stress response. *EMBO Rep*. 17(10): 1374-1395, 2016.

Papa SM, Desimone R, Fiorani M, Oldfield EH. Internal globus pallidus discharge is nearly suppressed during levodopa-induced dyskinesias. *Ann Neurol*. 46(5): 732-738, 1999.

Patten DA, Wong J, Khacho M, Soubannier V, Mailloux RJ, Pilon-Larose K, MacLaurin JG, Park DS, McBride HM, Trinkle-Mulcahy L, Harper ME, Germain M, Slack RS. OPA1-dependent cristae modulation is essential for cellular adaptation to metabolic demand. *EMBO J*. 33(22): 2676-2691, 2014.

Perese DA, Ulman J, Viola J, Ewing SE, Bankiewicz KS. A 6-hydroxydopamine-induced selective parkinsonian rat model. *Brain Res*. 494(2): 285-293, 1989.

Perciavalle RM, Opferman JT. Delving deeper: MCL-1's contributions to normal and cancer biology. *Trends Cell Biol*. 23(1): 22-29, 2013.

Perciavalle RM, Stewart DP, Koss B, Lynch J, Milasta S, Bathina M, Temirov J, Cleland MM, Pelletier S, Schuetz JD, Youle RJ, Green DR, Opferman JT. Anti-apoptotic MCL-1 localizes to the mitochondrial matrix and couples mitochondrial fusion to respiration. *Nat Cell Biol*. 14(6): 575–583, 2012.

Pickrell A, Huang C-H, Kennedy SR, Ordureau A, Sideris DP, Hoekstra JG, Harper JW, Youle RJ. Endogenous Parkin preserves dopaminergic Substantia Nigral neurons following mitochondrial DNA mutagenic stress. *Neuron*. 87(2): 371–381, 2015.

Protasoni M, Zeviani M. Mitochondrial structure and bioenergetics in normal and disease conditions. *Int J Mol Sci*. 22(2): 586, 2021.

Reeve A, Meagher M, Lax N, Simcox E, Hepplewhite P, Jaros E, Turnbull D. The impact of pathogenic mitochondrial DNA mutations on Substantia Nigra neurons. *J Neurosci*. 33(26): 10790-10801, 2013.

Robinson EJ, Aguiar SP, Kouwenhoven WM, Starmans DS, van Oerthel L, Smidt MP, van der Heide LP. Survival of midbrain dopamine neurons depends on the Bcl2 factor Mcl1. *Cell Death Discov*. 4: 107, 2018.

Rockenstein E, Mallory M, Hashimoto M, Song D, Shults CW, Lang I, Masliah E. Differential neuropathological alterations in transgenic mice expressing alpha-synuclein from the platelet-derived growth factor and Thy-1 promoters. *J Neurosci Res*. 68(5): 568-578, 2002.

Rodriguez-Sanchez F, Rodriguez-Blazquez C, Bielza C, Larrañaga P, Weintraub D, Martinez-Martin P, Rizos A, Schrag A, Chaudhuri KR. Identifying Parkinson's disease subtypes with motor and non-motor symptoms via model-based multi-partition clustering. *Sci Rep*. 11(1): 23645, 2021.

Rousseaux MW, Revelli JP, Vázquez-Vélez GE, Kim JY, Craigen E, Gonzales K, Beckinghausen J, Zoghbi HY. Depleting Trim28 in adult mice is well tolerated and reduces levels of α-synuclein and tau. *Elife*. 7: e36768, 2018.

Salazar C, Elorza AA, Cofre G, Ruiz-Hincapie P, Shirihai O, Ruiz LM. The OXPHOS supercomplex assembly factor HIG2A responds to changes in energetic metabolism and cell cycle. *J Cell Physiol*. 234(10): 17405-17419, 2019.

Sancho M, Leiva D, Lucendo E, Orzáez M. Understanding MCL1: from cellular function and regulation to pharmacological inhibition. *FEBS J*. DOI: 10.1111, 2021.

Servello D, Saleh C, Bona AR, Zekaj E, Zanaboni C, Porta M. Deep brain stimulation for Parkinson's disease prior to L-dopa treatment: A case report. *Surg Neurol Int*. 7(Suppl 35): S827-S829, 2013.

Shishido T, Nagano Y, Araki M, Kurashige T, Obayashi H, Nakamura T, Takahasi T, Matsumoto M, Maruyama H. Synphilin-1 has neuroprotective effects on MPP^+-induced Parkinson’s disease model cells by inhibiting ROS production and apoptosis. *Neurosci Lett*. 690: 145-150, 2019.

Sinha K, Joydeep D, Pal PB, Sil PC. Oxidative stress: the mitochondria-dependent and mitochondria-independent pathway of apoptosis. *Arch Toxicol*. 87(7): 1157-1180, 2013.

Smirnova E, Griparic L, Shurland DL, van der Bliek AM. Dynamin-related protein Drp1 is required for mitochondrial division in mammalian cells. *Mol Biol Cell*. 12(8): 2245-2256, 2001.

Song Z, Chen H, Fiket M, Alexander C, Chan DC. OPA1 processing controls mitochondrial fusion and is regulated by mRNA splicing, membrane potential, and Yme1L. *J Cell Biol*. 178(5): 749-55, 2007.

Song Z, Ghochani M, McCaffery JM, Frey TG, Chan DC. Mitofusins and OPA1 mediate sequential steps in mitochondrial membrane fusion. *Mol Biol Cell*. 20(15): 3525-3532, 2009.

Steimer DA, Boyd K, Takeuchi O, Fisher JK, Zambetti GP, Opferman JT. Selective roles for antiapoptotic MCL-1 during granulocyte development and macrophage effector function. *Blood*. 2009 Mar 19;113(12): 2805-2815, 2009.

Subramaniam SR, Chesselet MF. Mitochondrial dysfunction and oxidative stress in Parkinson's disease. *Prog Neurobiol*. 106-107: 17-32, 2013.

Sun X, Aimé P, Dai D, Ramalingam N, Crary JF, Burke RE, Greene LA, Levy OA. Guanabenz promotes neuronal survival via enhancement of ATF4 and parkin expression in models of Parkinson disease. *Exp Neurol*. 303: 95-107, 2018

Sun X, Liu J, Crary JF, Malagelada C, Sulzer D, Greene LA, Levy OA. ATF4 protects against neuronal death in cellular Parkinson's disease models by maintaining levels of parkin. *J Neurosci*. 33(6): 2398-2407, 2013.

Surinkaew P, Apaijai N, Sawaddiruk P, Jaiwongkam T, Kerdphoo S, Chattipakorn N, Chattipakorn SC. Mitochondrial fusion promoter alleviates brain damage in rats with cardiac ischemia/reperfusion injury. *J Alzheimers Dis*. 77(3): 993-1003, 2020.

Tardiolo G, Bramanti P, Mazzon E. Overview on the effects of *N*-acetylcysteine in neurodegenerative diseases. *Molecules*. 23(12): 3305, 2018.

Van Opdenbosch N, Lamkanfi M. Caspases in cell death, inflammation, and disease. *Immunity*. 50(6): 1352-1364, 2019.

Valente EM, Brancati F, Caputo V, Graham EA, Davis MB, Ferraris A, Breteler MM, Gasser T, Bonifati V, Bentivoglio AR, De Michele G, Dürr A, Cortelli P, Filla A, Meco G, Oostra BA, Brice A, Albanese A, Dallapiccola B, Wood NW; European Consortium on Genetic Susceptibility in Parkinson's Disease. PARK6 is a common cause of familial parkinsonism. *Neurol Sci*. 23 Suppl 2: S117-118, 2002.

Vassalli G, Büeler H, Dudler J, von Segesser LK, Kappenberger L. Adeno-associated virus (AAV) vectors achieve prolonged transgene expression in mouse myocardium and arteries in vivo: a comparative study with adenovirus vectors. *Int J Cardiol*. 90(2-3): 229-238, 2003.

Verfaillie T, Rubio N, Garg AD, Bultynck G, Rizzuto R, Decuypere J-P, Piette J, Linehan C, Gupta S, Samali A, Agostinis P. PERK is required at the ER-mitochondrial contact sites to convey apoptosis after ROS-based ER stress. *Cell Death Differ*. 19(11): 1880-1891, 2012.

Wang Y, Ebermann L, Sterner-Kock A, Wika S, Schultheiss HP, Dörner A, Walther T. Myocardial overexpression of adenine nucleotide translocase 1 ameliorates diabetic cardiomyopathy in mice. *Exp Physiol*. 94(2): 220-227, 2009.

Wang D, Wang J, Bonamy GM, Meeusen S, Brusch RG, Turk C, Yang P, Schultz PG. A small molecule promotes mitochondrial fusion in mammalian cells. *Angew Chem Int Ed Engl*. 51(37): 9302-9305, 2012.

Whitley BN, Engelhart EA, Hoppins S. Mitochondrial dynamics and their potential as a therapeutic target. *Mitochondrion*. 49: 269-283, 2019.

Willis SN, Chen L, Dewson G, Wei A, Naik E, Fletcher JI, Adams JM, Huang DC. Proapoptotic Bak is sequestered by Mcl-1 and Bcl-xL, but not Bcl-2, until displaced by BH3-only proteins. *Genes Dev*. 19(11): 1294-1305, 2005.

Wu S, Zhou F, Zhang Z, Xing D. Mitochondrial oxidative stress causes mitochondrial fragmentation via differential modulation of mitochondrial fission-fusion proteins. *FEBS J*. 278(6): 941-954, 2011.

Yang J, Kim KS, Iyirhiaro GO, Marcogliese PC, Callaghan SM, Qu D, Kim WJ, Slack RS, Park DS. DJ-1 modulates the unfolded protein response and cell death via upregulation of ATF4 following ER stress. *Cell Death Dis*. 10(2): 135, 2019.

Zamora M, Meroño C, Viñas O, Mampel T. Recruitment of NF-kappaB into mitochondria is involved in adenine nucleotide translocase 1 (ANT1)-induced apoptosis. *J Biol Chem*. 279(37): 38415-38423, 2004.

Zanna C, Ghelli A, Porcelli AM, Karbowski M, Youle RJ, Schimpf S, Wissinger B, Pinti M, Cossarizza A, Vidoni S, Valentino ML, Rugolo M, Carelli V. OPA1 mutations associated with dominant optic atrophy impair oxidative phosphorylation and mitochondrial fusion. *Brain*. 131(Pt 2): 352-367, 2008.

Zhang C, Jiang H, Wang P, Liu H, Sun X. Transcription factor NF-kappa B represses ANT1 transcription and leads to mitochondrial dysfunctions. *Sci Rep*. 7: 44708, 2017.

Zhang R, Li G, Zhang Q, Tang Q, Huang J, Hu C, Liu Y, Wang Q, Liu W, Gao N, Zhou S. Hirsutine induces mPTP-dependent apoptosis through ROCK1/PTEN/PI3K/GSK3β pathway in human lung cancer cells. *Cell Death Dis*. 9(6): 598, 2018.

Zhang J, Sun B, Yang J, Chen Z, Li Z, Zhang N, Li H, Shen L. Comparison of the effect of rotenone and 1-methyl-4-phenyl-1,2,3,6-tetrahydropyridine on inducing chronic Parkinson's disease in mouse models. *Mol Med Rep*. 25(3): 91, 2022.

Zhao RZ, Jiang S, Zhang L, Yu ZB. Mitochondrial electron transport chain, ROS generation and uncoupling (Review). *Int J Mol Med*. 44(1): 3-15, 2019.

Züchner S, Mersiyanova IV, Muglia M, Bissar-Tadmouri N, Rochelle J, Dadali EL, Zappia M, Nelis E, Patitucci A, Senderek J, Parman Y, Evgrafov O, Jonghe PD, Takahashi Y, Tsuji S, Pericak-Vance MA, Quattrone A, Battaloglu E, Polyakov AV, Timmerman V, Schröder JM, Vance JM. Mutations in the mitochondrial GTPase mitofusin 2 cause Charcot-Marie-Tooth neuropathy type 2A. *Nat Genet*. 36(5): 449-451, 2004.

APPENDICES

Appendix I: AAV cloning and production

AAV expression vector containing the cytomegalovirus enhancer/chicken β-actin promoter, a woodchuck post-transcriptional regulatory element, and the bovine growth hormone poly(A) was provided by Dr. Maxime Rousseaux (University of Ottawa) which was generated by Levites *et al*. (2006). The fluorescent tag mCherry was amplified by PCR from the pLVX-IRES-mCherry plasmid (Takara Bio; 631237). MCL1-OM and -Matrix fragments were generated by Twist Bioscience (San Francisco, CA, USA), fused to mCherry and linked to the porcine tecschovirus-1 2A (P2A) self-cleaving peptide. Primers and 2A sequences are found in **Table S1**. Fragments and the backbone were digested with EcoRI and BamHI, ligated, and transformed into DH5α *E. coli*. Plasmids were sequenced and tested in HEK293T cells prior to AAV production.

AAV REP/CAP packaging plasmid, pAAV2/8 (Addgene; 112864) was provided by Dr. James M. Wilson through Addgene. The pHelper packaging plasmid (Agilent; 240071) was provided by Dr. Maxime Rousseaux. AAV8 was generated in HEK293T cells by PEI co-transfection of the packaging plasmid, pHelper, and the gene of interest plasmids. Media was changed 24 hours post-transfection. Cells were harvested after 96 hours, briefly washed with 1X PBS, and lysed in 0.1% sodium deoxycholate. Then, 25 units of Benzonase were added to cell suspension, and incubated at 37°C for 30 min. Lysate was then centrifugated at 17,420 g, and supernatant was collected. AAV8 was purified through an Iodixanol (Millipore Sigma; D1556) gradient and washed 4X with 1X PBS. AAV8 was filtered through a 0.22 μm polyethersulfone (PES) filter, aliquoted, and stored at -80°C until use. To titre, AAV was lysed and quantified using qPCR using the method described in section 2.5. The region amplified was the bovine growth hormone (bGH) poly(A) sequence. Quantification was done by plotting against a serially diluted

standard curve which was derived from plasmids containing the bGH sequence. Primers are found in **Table S1**. Titre was expressed in genomic content (GC) per mL.

Cloning Primer	**Forward Sequence (5’ to 3’)**	**Reverse Sequence (5’ to 3’)**
mCherry	GAT CGG ATC CGC CAC CAT GGT GAG CAA GGG CGA G	GAT CGA ATT CTC ACT TGT ACA GCT CGT C
DNA Sequence	**Sequence (5’ to 3’)**	
P2A	GCT ACT AAC TTC AGC CTG CTG AAG CAG GCT GGA GAC GTG GAG GAG AAC CCT GGA CCT	
qPCR Sequence	**Forward Sequence (5’ to 3’)**	**Reverse Sequence (5’ to 3’)**
bGH Poly(A) Tail	TCC CAC TGT CCT TTC CTA	TGC CTG CTA TTG TCT TCC

Table S1: Primers and sequences used for AAV cloning

Appendix II: Permission to Reprint Published Figures

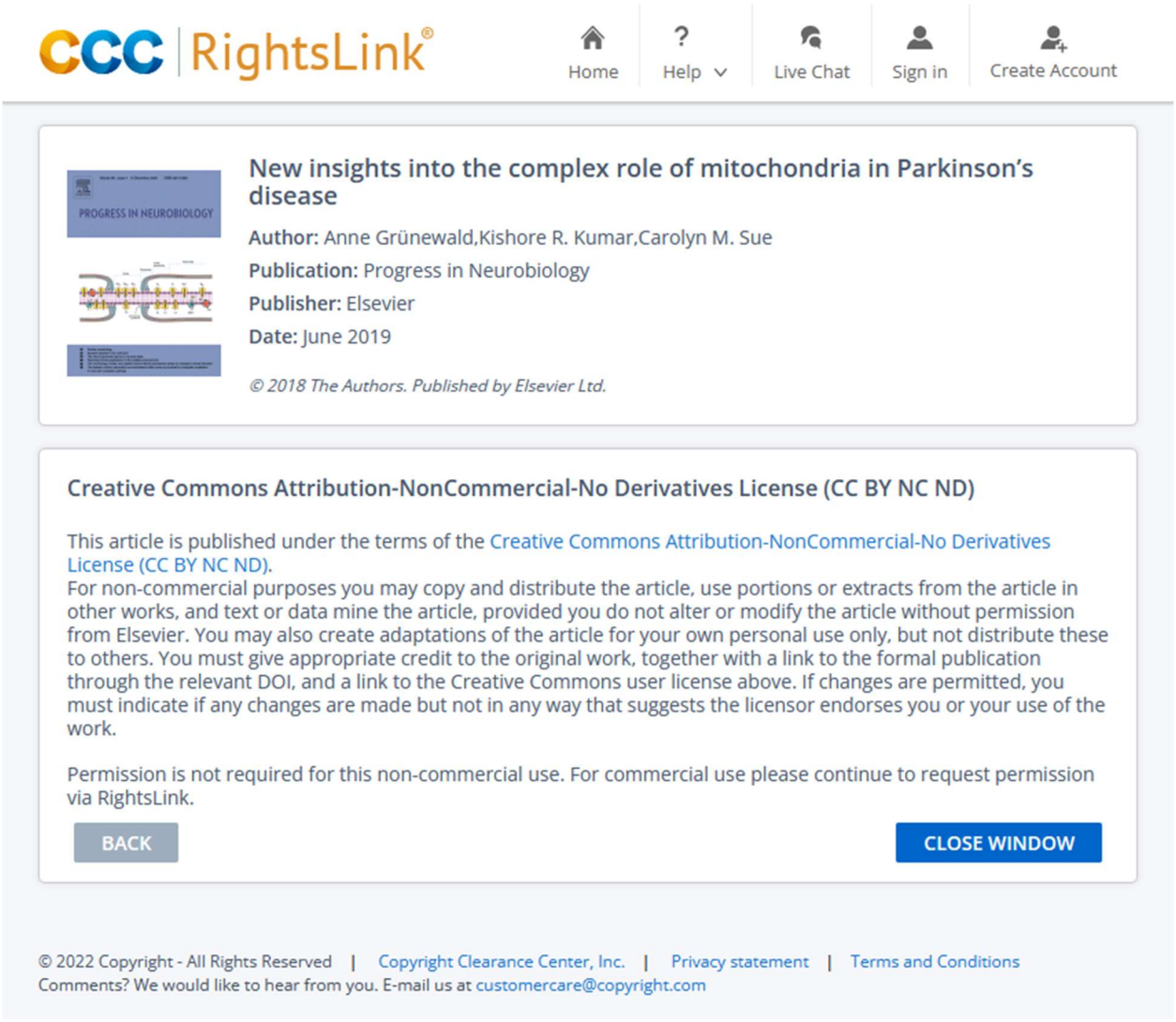

CCC | RightsLink®

Home | Help | Live Chat | Jingwei Chen

Delving deeper: MCL-1's contributions to normal and cancer biology

Author: Rhonda M. Perciavalle,Joseph T. Opferman
Publication: Trends in Cell Biology
Publisher: Elsevier
Date: January 2013

Order Completed

Thank you for your order.

This Agreement between Mr. Jingwei Chen ("You") and Elsevier ("Elsevier") consists of your license details and the terms and conditions provided by Elsevier and Copyright Clearance Center.

Your confirmation email will contain your order number for future reference.

Printable Details

License Number	5287180203098
License date	Apr 13, 2022

Licensed Content

Licensed Content Publisher	Elsevier
Licensed Content Publication	Trends in Cell Biology
Licensed Content Title	Delving deeper: MCL-1's contributions to normal and cancer biology
Licensed Content Author	Rhonda M. Perciavalle,Joseph T. Opferman
Licensed Content Date	Jan 1, 2013
Licensed Content Volume	23
Licensed Content Issue	1
Licensed Content Pages	8

Order Details

Type of Use	reuse in a thesis/dissertation
Portion	figures/tables/illustrations
Number of figures/tables /illustrations	1
Format	electronic
Are you the author of this Elsevier article?	No
Will you be translating?	No

About Your Work

Title	Manipulating mitochondrial integrity in a Parkinson's disease model
Institution name	University of Ottawa
Expected presentation date	Jul 2022

Additional Data

Portions	Figure 2 to be used in the introduction of the thesis

Requestor Location

Requestor Location	Mr. Jingwei Chen 451 Smyth Rd. Ottawa, ON K1H8M5 Canada Attn: Mr. Jingwei Chen

Tax Details

Publisher Tax ID	GB 494 6272 12

$ Price

Total	0.00 CAD

Total: 0.00 CAD

CLOSE WINDOW | ORDER MORE

CCC | RightsLink®

Home | Help | Live Chat | Jingwei Chen

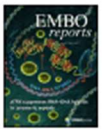

The integrated stress response

Author: Adrienne M Gorman, Afshin Samali, Mila Ljujic, et al
Publication: EMBO Reports
Publisher: John Wiley and Sons
Date: Sep 14, 2016

Order Completed

Thank you for your order.

This Agreement between Mr. Jingwei Chen ("You") and John Wiley and Sons ("John Wiley and Sons") consists of your license details and the terms and conditions provided by John Wiley and Sons and Copyright Clearance Center.

Your confirmation email will contain your order number for future reference.

License Number	5287180496655
License date	Apr 13, 2022

Printable Details

Licensed Content

Licensed Content Publisher	John Wiley and Sons
Licensed Content Publication	EMBO Reports
Licensed Content Title	The integrated stress response
Licensed Content Author	Adrienne M Gorman, Afshin Samali, Mila Ljujic, et al
Licensed Content Date	Sep 14, 2016
Licensed Content Volume	17
Licensed Content Issue	10
Licensed Content Pages	22

Order Details

Type of use	Dissertation/Thesis
Requestor type	University/Academic
Format	Electronic
Portion	Figure/table
Number of figures/tables	1
Will you be translating?	No

About Your Work

Title	Manipulating mitochondrial integrity in a Parkinson's disease model
Institution name	University of Ottawa
Expected presentation date	Jul 2022

Additional Data

Portions	Figure 1 to be used in the introduction of the thesis

Requestor Location

Requestor Location	Mr. Jingwei Chen 451 Smyth Rd. Ottawa, ON K1H8M5 Canada Attn: Mr. Jingwei Chen

Tax Details

Publisher Tax ID	EU826007151

$ Price

Total	0.00 CAD

Would you like to purchase the full text of this article? If so, please continue on to the content ordering system located here: Purchase PDF
If you click on the buttons below or close this window, you will not be able to return to the content ordering system.

Total: 0.00 CAD

CLOSE WINDOW | ORDER MORE